The transcription factor Zeb2 drives differentiation of age-associated B cells

Shuangshuang Gu[1, 8], Xiaxia Han[1, 8], Chao Yao[6, 8], Huihua Ding[1], Jinsong Zhang[6], Guojun Hou[1], Bo Qu[1], Haibo Zhou[1], Zhihua Ying[3], Zhizhong Ye[3], Jie Qian[1], Qiang Guo[1], Sheng Chen[1], Carola G. Vinuesa[2, 7, *], Dai Dai[1, *], Nan Shen[1, 2, 3, 4, 5, 9,*]

[1] Shanghai Institute of Rheumatology, Shanghai Renji Hospital, Shanghai Jiaotong University School of Medicine, Shanghai, 200001, China.

[2] Centre for Personalised Immunology (CACPI), Renji Hospital, School of Medicine, Shanghai Jiao Tong University (SJTUSM), Shanghai, 200001, China.

[3] Shenzhen Futian Hospital for Rheumatic Diseases, Shenzhen, 518000, China.

[4] State Key Laboratory of Oncogenes and Related Genes, Shanghai Cancer Institute, Renji Hospital, Shanghai Jiaotong University School of Medicine, Shanghai, 200001, China.

[5] Center for Autoimmune Genomics and Etiology (CAGE) and Divisions of Rheumatology, Cincinnati Children's Hospital Medical Center, Cincinnati OH 45229, USA.

[6] Shanghai Institute of Nutrition and Health, University of Chinese Academy of Sciences, Chinese Academy of Sciences, Shanghai 200031, China.

[7] Centre for Personalised Immunology, John Curtin School of Medical Research, Australian National University, 131 Garran Rd, Acton, 2601, ACT, Australia.

[8] These authors contributed equally to the work

*Correspondence to:

Nan Shen: nanshensibs@gmail.com

Dai Dai: daidaisibs@163.com

Carola G. Vinuesa: carola.vinuesa@anu.edu.au

Abstract

Age-associated B cells (ABCs) accumulate after infection, during aging, and in systemic autoimmunity, contributing to pathogenesis in the latter[1]. To date, their precise ontogeny and whether they represent a B cell subset distinct from the other major effector subsets - plasma cells and memory B cells - remain unknown. We asked whether ABC formation requires the expression of a unique transcription factor. Here, we used single-cell RNA sequencing to identify differentially-expressed transcription factors shared by ABCs from both lupus patient and lupus-prone mice. Using an arrayed CRISPR screen, we show Zeb2 is essential for ABC differentiation in vitro. Selective deficiency of Zeb2 in B cells also leads to impaired ABC formation in vivo. Zeb2 drove ABC specification by directly binding the promoters of ABC signature genes including *Itgax* and *Itgam* encoding for CD11c and CD11b respectively. Zeb2 also targeted molecules involved in cytokine receptor signaling via the JAK/STAT pathway including *Il21r* and *Socs5*. Administration of the approved JAK/STAT inhibitor tofacitinib effectively ameliorated ABC accumulation in mice and patients with autoimmunity. This study reveals ABCs represent a distinct B cell subset dependent on Zeb2 expression, and provides a rationale for the use of JAK/STAT inhibitors to treat ABC-mediated autoimmune diseases.

Main

Age-associated B cells (ABC) characterized by high expression of CD11c and T-bet are found at increased numbers in aged female mice, infection models and multiple autoimmune diseases[1]. This novel B cell subset has been given various names including ABCs, CD11c$^+$ B cells, CD11c$^+$T-bet$^+$ B cells, CD21$^-$CD23$^-$B cells, Be1 cells, double negative B cells (DN), DN2 or atypical memory B cells[2-10]. ABCs or ABC-like B cells identified as CD11c$^+$ T-bet$^+$CD11b$^+$CD21$^-$CD23$^-$CD86^{hi}MHCII^{hi}CD95$^+$ in mice[2,8] and CD11c$^+$T-bet$^+$CD27$^-$IgD$^-$CD38$^-$CD21$^-$CD95^{hi}FCRL5$^+$ in humans[4,6] will be referred to as ABCs henceforth, following the suggestion of a recent review[1]. In autoimmune settings, these B cells are enriched for autoantibody specificities. It is widely accepted that these cells are antigen-experienced and it has been suggested that they can rapidly differentiate into antibody-secreting cells (ASCs) upon antigen reencounter or innate stimulation[11,12].

The transcriptional factor T-bet is highly expressed in ABCs and it is required for autoantibody production in lupus-prone mice[3,13]. T-bet has been put forward as a functional regulator of ABC differentiation by putatively binding *Il21r* promoters in humans[9] and by suppressing an IFN-γ-induced inflammatory network that supports ABC terminal differentiation to ASCs in mice[10]. However, T-bet is dispensable for ABC formation or maintenance of ABC features[14,15] arguing against it being the master regulator of ABCs. In search for the TF essential for ABC formation, we screened all TFs expressed by these cells and identified Zeb2 as the key regulator required for ABC specification and differentiation in mouse and human.

Differentially-expressed TFs in autoimmune ABCs

To gain insights into the nature of ABCs, we sorted peripheral B cells from a patient with new-onset SLE (Supplementary Table 1) and performed droplet-based scRNA-seq. Seven distinct clusters containing from 94 to 1640 cells

were revealed by unsupervised clustering with a two-dimensional uniform manifold approximation and projection (UMAP) (Fig. 1a and Extended Data Fig. 1b). These clusters were assigned to known peripheral B cell subsets including transitional B cells (TrB), naïve B cells (NavB), activated naïve B cells (aNavB), ABCs, memory B cells (MemB), plasmablasts (PB) and plasma cells (PC) by comparing DEGs with established markers and previously described gene expression profiles[6,16,17]. Landmark genes (*IGHD*, *CD27*, *CD38*, *CD24*, *CD9*, *CD79B*, *VPREB3*, *MZB1*, *PRDM1*, *XBP1*, *IRF4*, *PCNA*, *MKI67*, *IGHG1*, *IGHF3*, *IGKC*, *JCHAIN*) were used to identify clusters (Extended Data Fig. 1a, c).

ABCs preferentially expressed genes encoding key surface markers: *ITGAX*, *CD19*, *MS4A1*, *CD86*, *FCRLA*, *FCRL3/5* and *FCGRB2,* and they lacked *CR2*, *FCER2*, *CD27* and *IGHD* (Fig. 1b). Amongst transcripts encoding chemokine receptors, *CXCR3* was highly expressed while *CXCR4* and *CXCR5* were suppressed. Besides these, we identified 43 differentially-expressed TFs in ABCs: 27 upregulated (*HOPX*, *ZEB2*, *POU2F2*, *TOX*, *KLF3*, *ARID3A*, *TBX21*, *LITAF*, *PLEK*, *ZBTB32*, *TFEB*, *NR4A2*, *NFATC2*, *SREBF2*, *TOX2*, *JUN*B, *ZNF331*, *BATF*, *KLF6*, *TFEC*, *CREM*, *BHLHE40*, *SOX5*, *JUN*, *JAZF1*, *FOXP4*, *ARID5A*) and 16 downregulated (*HIF1A*, *MBD4*, *ETS1*, *SP140L*, *FLI1*, *ZNF92*, *ZFP36L1*, *PLSCR1*, *AFF3*, *IRF8*, *FOS*, *MYC*, *FOXP1*, *ZFP36L2*, *IRF1*, *BACH2*) (Fig. 1c).

We previously reported T-bet^{+}CD11c^{+} B cells accumulate in Bm12-induced lupus and contribute to autoantibody production[3]. Whether Bm12-induced T-bet^{+}CD11c^{+} B cells represent *bona fide* ABCs has not been described. Flow cytometric staining revealed that CD11c^{+} B cells from Bm12-induced mice exhibited ABC-specific features including a hyperactivated state (CD19^{hi}CD86^{hi}CD62L^{low}CD44^{hi}CD95^{hi}MHCII^{hi}), characteristic markers (CD11c^{+}T-bet^{hi} CD11b^{hi}), specific lineage association (CD23^{-}CD21^{-}CD93^{-} CD5^{int}CD138^{-}IgD^{low}IgM^{int}) and elevated expression of chemokine receptors

111 CXCR3 and CXCR4 (Fig. 1d). We used the surface marker CD21 to exclude
112 the small fraction of naive CD11c$^+$ B cells. Consistent with previous reports,
113 Bm12-indued CD11c$^+$ CD21$^-$ B cells expressed high amounts of *Cxcl9* and
114 *Cxcl10* transcripts (Fig. 1e). We then used qPCR to validate 40 differentially-
115 expressed TFs identified in our human scRNA-seq data excluding *ZNF331*,
116 *SP140L* and *ZNF92*, which lack orthologs in mice (Fig.1f). Amongst these, 13
117 upregulated TFs (*Tbx21*, *Zeb2*, *Plek*, *Litaf*, *Tfeb*, *Nfatc2*, *Zbtb32*, *Srebf2*, *Jazf1*,
118 *Jun*, *Sox5*, *Tfec*, *Batf*) and 3 downregulated TFs (*Ets1*, *Mbd4*, *Fli1*) were
119 identically regulated in human and mouse ABCs and were therefore considered
120 potential transcriptional regulators of ABC differentiation.
121
122 **Screen for TFs directing mouse ABC differentiation**
123 ABCs can be generated in vitro[10,18] and TLR signaling, BCR engagement, T
124 cell help and the T cell-derived cytokines IFN-γ and IL-21 have been shown to
125 be important for ABC formation in ageing, infection and autoimmune
126 settings[2,5,15,18,19]. We investigated the optimal combination of stimuli for efficient
127 ABC induction within 3 days of culture (Fig. 2a and Extended Data Fig. 2a-d).
128 BCR engagement with anti-CD40 and R848 promoted B cell viability (Extended
129 Data Fig. 2a, b). IL-21 induced CD11c and T-bet expression while IFN-γ only
130 facilitated T-bet expression (Extended Data Fig. 2d, e). IL-21 and IFN-γ
131 signaling could enhance *Cd86*, *Cxcr3* and *Cxcl10* expression (Extended Data
132 Fig. 2e). We therefore used a cocktail of anti-IgM, R848, anti-CD40, IL-21 and
133 IFN-γ for in vitro ABC induction.
134
135 To screen for functional transcriptional regulators of ABC differentiation, B cells
136 from Cas9 transgenic mice and congenic CD45.1 mice were cocultured in a 4:1
137 ratio and activated with anti-IgM, anti-CD40 and R848 for 24 hours. B cells
138 expressing CD45.1 and lacking Cas9 were transduced with sgRNA plasmids
139 and served as controls in these co-cultures. Activated B cells were then
140 retrovirally infected with the sgRNA plasmids co-expressed with the blue

141 fluorescent protein (BFP), and cultured for a further 3 days with the ABC
142 differentiation cocktail (Fig. 2b). We then compared the ratio between live
143 BFP$^+$CD45.1$^-$ (Cas9$^+$, edited) and BFP$^+$CD45.1$^+$ (Cas9$^-$, unedited) CD11c$^+$T-
144 bet$^+$ ABCs (Extended Data Fig. 3a). To validate our genome editing tools we
145 introduced a sgRNA sequence specific for *Itgax* and showed effective blockade
146 of CD11c$^+$T-bet$^+$ ABC cell formation from Cas9$^+$ B cells (Extended Data Fig. 3b).
147 We then screened the 16 candidate TFs and identified 7 (T-bet, Batf, Ets1, Fli1,
148 Jun, Srebf2, Zeb2) that could significantly ($P<0.05$) alter ABC formation (Fig. 2c
149 and Extended Data Fig. 3c). Except for Zeb2, ablation of the other 6 TFs
150 predominantly influenced cell viability (Extended Data Fig. 3d). Two different
151 sgRNAs targeting *Zeb2* in separate Cas9$^+$ B cell cultures lead to reduced ABC
152 formation (Fig. 2d), which excluded an off-target editing effect. Taken together,
153 we identify 7 functional TFs required for mouse ABC differentiation, with one of
154 them, Zeb2, acting by means other than promoting cell survival.
155
156 **Functional assessment of candidate TFs in human ABCs**
157 We next set out to determine whether besides Zeb2, any of the other 6 TFs was
158 required for human ABC lineage specification, using an established in vitro ABC
159 induction protocol used in human studies[4,6,9] (Fig. 2e). Synergistic stimulation
160 with anti-Ig, R848, BAFF, IL-2, anti-CD40, IL-21 and IFN-γ increased IgD$^-$CD27$^-$
161 DN and CD11c$^+$ T-bet$^+$ ABC percentages with a high B cell survival rate (>70%)
162 (Extended Data Fig. 4a-d). Compared with naïve and switched B cells, in vitro-
163 derived DN B cells contained the highest frequency of CD11c$^+$T-bet$^+$ cells
164 (Extended Data Fig. 4e, f).
165
166 We next transduced Cas9-guide RNA ribonucleoprotein (RNP) complexes by
167 electroporation to edit genes in primary human B cells. Using a sgRNA
168 sequence targeting *CD19* as a positive control, we achieved extremely efficient
169 gene disruption (Extended Data Fig. 5a). Primary B cells were isolated and
170 purified from the blood of healthy individuals. After activation for one day, cells

171 were electroporated with RNP and treated with the ABC differentiation cocktail
172 for another 3 days (Extended Data Fig. 5b). All of the 7 TFs identified in mice
173 led to changes in human ABC's when individually ablated ($P<0.05$) (Fig. 2f,g
174 and Extended Data Fig. 5c). Two different guide RNAs targeting *ZEB2* achieved
175 reduced T-bet expression (Fig. 2h). Gene editing of *ETS1*, *FLI1* and *JUN* had
176 opposite effects on human ABCs and were excluded. Ablation of *TBX21*, *ZEB2*,
177 *BATF* and *SREBF2* dampened ABC differentiation in both human and mouse
178 B cells. However, *TBX21*, *BATF* and *SREBF2* deficiency also impaired human
179 cell viability (Extended Data Fig. 5d, e). As a key regulator of lipid metabolism,
180 SREBF2 is required to supply lipids for membrane synthesis and has been
181 reported to influence T cell survival and the GC response[20,21]. Although there is
182 no published evidence that T-bet and BATF control B cell proliferation or death,
183 both TFs have been implicated in B lymphoproliferative disorders[22,23]. After
184 exclusion of the genes predominantly affecting cell viability, Zeb2 emerged as
185 the single TF with consistent regulatory effects in human and mouse ABC
186 formation and therefore the key ABC transcriptional regulator.
187
188 **Zeb2 is required for ABC formation**
189 Zeb2 belongs to the zinc-finger E homeobox-binding protein family and is
190 known to drive epithelial to mesenchymal transition in cancer progression[24]. In
191 the immune system, Zeb2 has been reported to be expressed in dendritic cells
192 (DC), macrophages, B, T and NK cells and participate in transcriptional
193 networks involved in cell differentiation, maintenance and function[25-33]. To
194 further explore how Zeb2 deficiency affects ABC formation we generated mice
195 selectively lacking Zeb2 in B cells by crossing Zeb2 floxed mice with CD19-cre
196 mice (Extended Data Fig. 6a-c). We first isolated B cells from $Zeb2^{f/f}CD19^{cre/+}$
197 conditional knockout mice (CKO) and $Zeb2^{f/f}$ littermate control mice (Ctrl) and
198 induced in vitro ABC differentiation for 3 days. Zeb2 deficiency significantly
199 impaired ABC differentiation (Fig. 3a). Zeb2 deficient B cells also exhibited
200 decreased CD11c and T-bet expression (Extended Data Fig. 6d, e).

201

202 We then investigated the *in vivo* effects of Zeb2 ablation in B cells on ABC
203 formation, using the Bm12-induced lupus model. As early as 2 weeks after
204 adoptive transfer of CD4+ T cell from Bm12 mice, the proportion of ABC cells
205 identified as $CD11c^{+}CD11b^{+}T\text{-}bet^{+}CD21^{-}$ or $CD21^{-}CD23^{-}CD11c^{+}CD11b^{+}$ was
206 significantly reduced in Zeb2 CKO mice (Fig. 3b, c). The absolute number of
207 ABCs was reduced by over 50% in Zeb2 CKO mice. By contrast, no differences
208 in the numbers of GC B cells or plasma cells were seen in Zeb2 CKO mice
209 (Extended Data Fig. 6f, g), reflecting a specific regulatory role of Zeb2 in ABC
210 formation. These results confirm that Zeb2 deficiency in B cells leads to
211 impaired ABC formation both in vitro and in vivo.

212

213 **Zeb2 directly regulates ABC signature genes**

214 The mechanisms involved in Zeb-mediated gene regulation are broad and cell-
215 context specific[25,26,28,31]. To investigate the consequences of Zeb2 regulation of
216 gene transcription we performed RNA sequencing on sorted B cells with
217 reduced Zeb2 (sg-*Zeb2* ($CD19^{+}GFP^{+}BFP^{+}$)) or T-bet (sg-*Tbx21)* expression 4
218 days after in vitro activation, retroviral infection and differentiation (Extended
219 Data Fig. 7a). We found sg-*Zeb2* B cells expressed less *Il7r* consistent with
220 reports of Zeb2-mediated regulation of IL-7R expression during pro-pre B cell
221 development[30] (Fig. 4a). Comparative analysis identified that ABC signature
222 genes *Itgax*, *Tbx21*, *Itgam*, *Cxcr4* and *Cxcl10* were downregulated while *Fcer2a*
223 (encoding CD23a) was upregulated in sg-*Zeb2* B cells (Fig. 4a, b). In vitro-
224 derived ABCs from Zeb2 CKO mice also lacked expression of ABC signature
225 genes including *Itgax*, *Itgam* and *Cxcr4* (Extended Data Fig. 7e). T-bet ablation
226 also impaired some aspects of the ABC phenotype (Fig. 4b and Extended Data
227 Fig. 7b). Principal component analysis (PCA) distinctly separated sg-*Zeb2* and
228 sg-*Tbx21* B cells suggesting different regulatory roles for these two TFs during
229 ABC differentiation (Extended Data Fig. 7c). Clustering by signature genes
230 revealed Zeb2 ablation resulted in more severe impairment of ABC identity

231 compared with T-bet ablation (Fig. 4b).

232

233 To determine the direct gene targets of Zeb2 regulation, we performed cleavage
234 under targets and tagmentation (Cut & tag) followed by sequencing the
235 enriched DNA fragments[34]. Cut & tag-seq signals were compared among Zeb2
236 specific, T-bet specific and IgG peaks. Zeb2 signals were enriched in the
237 transcriptional start sites (TSS) especially within promoter regions (Extended
238 Data Fig. 8a, b). Zeb2 specific peaks were matched to motifs of Gata3, Fosl2
239 and Zeb2 (Extended Data Fig. 8c), consistent with Zeb2 Chip-seq data in cell
240 lines from the Encode project (Extended Data Fig. 8e). We found the
241 transcriptional regulatory regions of *Itgax* and *Itagm* were enriched in Zeb2-
242 specific peaks and these loci contained a Zeb2 binding motif (Fig. 4c). These
243 results suggest that Zeb2 orchestrates ABC specification by directly targeting
244 ABC signature genes including *Itgax* and *Itgam*.

245

246 **Zeb2-Jak-Stat axis controls ABC differentiation**

247 KEGG analysis revealed that the top pathway of downregulated genes in sg-
248 *Zeb2* cells was related to Jak-Stat signaling (Extended Data Fig. 7d). Signaling
249 landscape changes downstream of cytokine receptor signaling via Jak-Stat
250 were annotated (Fig. 4a) and genes involved in Jak-Stat signaling with
251 significant changes were listed in a heatmap (Fig. 4d). Gene set enrichment
252 analysis (GSEA) also revealed sg-Zeb2 B cells had altered Jak-Stat signaling
253 (Fig. 4e), which is known to be critical for ABC differentiation[1]. We validated
254 differentially-expressed genes involved in Jak-Stat signaling using in vitro-
255 derived ABCs from Zeb2 CKO mouse B cells (Extended Data Fig. 7e). There
256 was a positive correlation between *IL21R* and *ZEB2* expression in B cells from
257 SLE patients (Extended Data Fig. 7f). We then compared DEGs with Zeb2
258 specific signals from cut-tag to narrow down the key direct targets in Jak-Stat
259 pathways. The promoters of *Socs5* and *Il21r* were enriched in the Zeb2-specific
260 group. These loci also contained Zeb2 binding motifs (Extended Data Fig. 8f).

261 SOCS5 is a negative regulator of IL-4 / STAT6 signaling, which dampens ABC
262 formation[18]. IL-21 signaling via IL21R is critical for ABC differentiation[4,18]. These
263 results suggest that Zeb2 directly regulates important components of Jak-Stat
264 signaling including *Socs5* and *Il21r* to drive ABC differentiation.
265
266 Jak-Stat inhibitors have proven to be a safe and efficient strategy to dampen
267 intracellular cytokine signaling[35]. Baricitinib, tofacitinib, upadacitinib and
268 filgotinib have been approved for oral therapy in rheumatoid arthritis (RA) and
269 are also commonly prescribed off-label in other autoimmune diseases including
270 SLE, inflammatory bowel disease and psoriasis[36]. We therefore investigated
271 the effects of Jak-Stat inhibitors on ABC formation. Baricitinib or tofacitinib
272 impaired mouse in vitro ABC differentiation in a dose-dependent manner (Fig.
273 4f and Extended Data Fig. 9a-d). Oral administration of tofacitinib reduced
274 splenomegaly and autoantibody titers in the Bm12-induced lupus model
275 (Extended Data Fig. 9e-g). Notably, accumulation of ABCs was effectively
276 ameliorated by tofacitinib (Fig. 4g). Accordingly, human ABC differentiation in
277 vitro was also blocked by baricitinib and tofacitinib (Fig 4h and Extended Data
278 Fig. 9h). Finally, we investigated the *in vivo* effects of tofacitinib on ABC
279 differentiation in RA patients. The frequency of human ABCs (DN2) had
280 decreased 4 weeks after treatment (Fig. 4i). Tofacitinib also ameliorated
281 systemic inflammation lowering C-reactive protein (CRP) (Extended Data Fig.
282 9i). These results clearly demonstrate that targeting the Jak-Stat pathway is an
283 efficient strategy to block ABCs in mice and humans and provide a rationale for
284 the use of Jak-Stat inhibition therapy in ABC-mediated autoimmunity.
285
286 In summary, our results have identified Zeb2 as an essential TF that regulates
287 human and mouse ABC differentiation by targeting Jak-Stat signaling.
288 Surprisingly, Zeb2 rather than T-bet, determines ABC specification. Mice and
289 humans have ABC subsets that share a similar phenotype and exert pathogenic
290 roles in autoimmunity[1]. It is therefore not surprising that both require Zeb2 for

ABC development. Although our TF screen takes advantage of an autoimmune model for rapid ABC development, our results are likely to apply to other settings as ABCs have been shown to be comparable in the context of ageing, infection and autoimmunity.

296 **References**

297 1 Cancro, M. P. Age-Associated B Cells. *Annu Rev Immunol* **38**, 315-
298 340, doi:10.1146/annurev-immunol-092419-031130 (2020).
299 2 Rubtsov, A. V. *et al.* Toll-like receptor 7 (TLR7)-driven accumulation of a
300 novel CD11c(+) B-cell population is important for the development of
301 autoimmunity. *Blood* **118**, 1305-1315, doi:10.1182/blood-2011-01-
302 331462 (2011).
303 3 Liu, Y. *et al.* T-bet+CD11c+ B cells are critical for antichromatin
304 immunoglobulin G production in the development of lupus. *Arthritis*
305 *Research & Therapy* **19**, doi:10.1186/s13075-017-1438-2 (2017).
306 4 Wang, S. *et al.* IL-21 drives expansion and plasma cell differentiation of
307 autoreactive CD11c(hi)T-bet(+) B cells in SLE. *Nat Commun* **9**, 1758,
308 doi:10.1038/s41467-018-03750-7 (2018).
309 5 Manni, M. *et al.* Regulation of age-associated B cells by IRF5 in
310 systemic autoimmunity. *Nat Immunol* **19**, 407-419, doi:10.1038/s41590-
311 018-0056-8 (2018).
312 6 Jenks, S. A. *et al.* Distinct Effector B Cells Induced by Unregulated Toll-
313 like Receptor 7 Contribute to Pathogenic Responses in Systemic
314 Lupus Erythematosus. *Immunity* **49**, 725-739 e726,
315 doi:10.1016/j.immuni.2018.08.015 (2018).
316 7 Wu, C. *et al.* Lupus-associated atypical memory B cells are mTORC1-
317 hyperactivated and functionally dysregulated. *Ann Rheum Dis* **78**,
318 1090-1100, doi:10.1136/annrheumdis-2019-215039 (2019).
319 8 Hao, Y., O'Neill, P., Naradikian, M. S., Scholz, J. L. & Cancro, M. P. A B-
320 cell subset uniquely responsive to innate stimuli accumulates in aged
321 mice. *Blood* **118**, 1294-1304, doi:10.1182/blood-2011-01-330530
322 (2011).
323 9 Zumaquero, E. *et al.* IFNgamma induces epigenetic programming of
324 human T-bet(hi) B cells and promotes TLR7/8 and IL-21 induced
325 differentiation. *Elife* **8**, doi:10.7554/eLife.41641 (2019).
326 10 Stone, S. L. *et al.* T-bet Transcription Factor Promotes Antibody-
327 Secreting Cell Differentiation by Limiting the Inflammatory Effects of
328 IFN-gamma on B Cells. *Immunity* **50**, 1172-1187 e1177,
329 doi:10.1016/j.immuni.2019.04.004 (2019).
330 11 Myles, A., Sanz, I. & Cancro, M. P. T-bet(+) B cells: A common
331 denominator in protective and autoreactive antibody responses? *Curr*
332 *Opin Immunol* **57**, 40-45, doi:10.1016/j.coi.2019.01.002 (2019).
333 12 Rubtsov, A. V., Marrack, P. & Rubtsova, K. T-bet expressing B cells -
334 Novel target for autoimmune therapies? *Cell Immunol* **321**, 35-39,
335 doi:10.1016/j.cellimm.2017.04.011 (2017).
336 13 Rubtsova, K. *et al.* B cells expressing the transcription factor T-bet
337 drive lupus-like autoimmunity. *J Clin Invest* **127**, 1392-1404,
338 doi:10.1172/JCI91250 (2017).
339 14 Du, S. W., Arkatkar, T., Jacobs, H. M., Rawlings, D. J. & Jackson, S. W.
340 Generation of functional murine CD11c(+) age-associated B cells in the
341 absence of B cell T-bet expression. *Eur J Immunol* **49**, 170-178,
342 doi:10.1002/eji.201847641 (2019).
343 15 Levack, R. C., Newell, K. L., Popescu, M., Cabrera-Martinez, B. &
344 Winslow, G. M. CD11c(+) T-bet(+) B Cells Require IL-21 and IFN-

gamma from Type 1 T Follicular Helper Cells and Intrinsic Bcl-6 Expression but Develop Normally in the Absence of T-bet. *J Immunol* **205**, 1050-1058, doi:10.4049/jimmunol.2000206 (2020).

16 Kaminski, D. A., Wei, C., Qian, Y., Rosenberg, A. F. & Sanz, I. Advances in human B cell phenotypic profiling. *Front Immunol* **3**, 302, doi:10.3389/fimmu.2012.00302 (2012).

17 Glass, D. R. *et al.* An Integrated Multi-omic Single-Cell Atlas of Human B Cell Identity. *Immunity* **53**, 217-232.e215, doi:10.1016/j.immuni.2020.06.013 (2020).

18 Naradikian, M. S. *et al.* Cutting Edge: IL-4, IL-21, and IFN-gamma Interact To Govern T-bet and CD11c Expression in TLR-Activated B Cells. *J Immunol* **197**, 1023-1028, doi:10.4049/jimmunol.1600522 (2016).

19 Russell Knode, L. M. *et al.* Age-Associated B Cells Express a Diverse Repertoire of VH and Vkappa Genes with Somatic Hypermutation. *J Immunol* **198**, 1921-1927, doi:10.4049/jimmunol.1601106 (2017).

20 Kidani, Y. *et al.* Sterol regulatory element-binding proteins are essential for the metabolic programming of effector T cells and adaptive immunity. *Nat Immunol* **14**, 489-499, doi:10.1038/ni.2570 (2013).

21 Ricker, E. *et al.* Serine-threonine kinase ROCK2 regulates germinal center B cell positioning and cholesterol biosynthesis. *J Clin Invest* **130**, 3654-3670, doi:10.1172/jci132414 (2020).

22 Dorfman, D. M., Hwang, E. S., Shahsafaei, A. & Glimcher, L. H. T-bet, a T-Cell–Associated Transcription Factor, Is Expressed in a Subset of B-Cell Lymphoproliferative Disorders. *American Journal of Clinical Pathology* **122**, 292-297, doi:10.1309/aqq2dvm75dvy0pwp (2004).

23 Care, M. A. *et al.* SPIB and BATF provide alternate determinants of IRF4 occupancy in diffuse large B-cell lymphoma linked to disease heterogeneity. *Nucleic Acids Res* **42**, 7591-7610, doi:10.1093/nar/gku451 (2014).

24 Vandewalle, C. *et al.* SIP1/ZEB2 induces EMT by repressing genes of different epithelial cell-cell junctions. *Nucleic Acids Res* **33**, 6566-6578, doi:10.1093/nar/gki965 (2005).

25 Bagadia, P. *et al.* An Nfil3-Zeb2-Id2 pathway imposes Irf8 enhancer switching during cDC1 development. *Nat Immunol* **20**, 1174-1185, doi:10.1038/s41590-019-0449-3 (2019).

26 Scott, C. L. *et al.* The transcription factor Zeb2 regulates development of conventional and plasmacytoid DCs by repressing Id2. *J Exp Med* **213**, 897-911, doi:10.1084/jem.20151715 (2016).

27 Wu, X. *et al.* Transcription factor Zeb2 regulates commitment to plasmacytoid dendritic cell and monocyte fate. *Proc Natl Acad Sci U S A* **113**, 14775-14780, doi:10.1073/pnas.1611408114 (2016).

28 Dominguez, C. X. *et al.* The transcription factors ZEB2 and T-bet cooperate to program cytotoxic T cell terminal differentiation in response to LCMV viral infection. *J Exp Med* **212**, 2041-2056, doi:10.1084/jem.20150186 (2015).

29 Omilusik, K. D. *et al.* Transcriptional repressor ZEB2 promotes terminal differentiation of CD8+ effector and memory T cell populations during infection. *J Exp Med* **212**, 2027-2039, doi:10.1084/jem.20150194 (2015).

30 Li, J. *et al.* The EMT transcription factor Zeb2 controls adult murine hematopoietic differentiation by regulating cytokine signaling. *Blood* **129**, 460-472, doi:10.1182/blood-2016-05-714659 (2017).
31 Scott, C. L. *et al.* The Transcription Factor ZEB2 Is Required to Maintain the Tissue-Specific Identities of Macrophages. *Immunity* **49**, 312-325 e315, doi:10.1016/j.immuni.2018.07.004 (2018).
32 Collins, P. L. *et al.* Gene Regulatory Programs Conferring Phenotypic Identities to Human NK Cells. *Cell* **176**, 348-360 e312, doi:10.1016/j.cell.2018.11.045 (2019).
33 Huang, X. *et al.* Differential usage of transcriptional repressor Zeb2 enhancers distinguishes adult and embryonic hematopoiesis. *Immunity*, doi:10.1016/j.immuni.2021.04.015 (2021).
34 Kaya-Okur, H. S. *et al.* CUT&Tag for efficient epigenomic profiling of small samples and single cells. *Nat Commun* **10**, 1930, doi:10.1038/s41467-019-09982-5 (2019).
35 O'Shea, J. J., Kontzias, A., Yamaoka, K., Tanaka, Y. & Laurence, A. Janus kinase inhibitors in autoimmune diseases. *Ann Rheum Dis* **72 Suppl 2**, ii111-115, doi:10.1136/annrheumdis-2012-202576 (2013).
36 Traves, P. G. *et al.* JAK selectivity and the implications for clinical inhibition of pharmacodynamic cytokine signalling by filgotinib, upadacitinib, tofacitinib and baricitinib. *Ann Rheum Dis*, doi:10.1136/annrheumdis-2020-219012 (2021).
37 Klarquist, J. & Janssen, E. M. The bm12 Inducible Model of Systemic Lupus Erythematosus (SLE) in C57BL/6 Mice. *J Vis Exp*, e53319, doi:10.3791/53319 (2015).
38 Cossarizza, A. *et al.* Guidelines for the use of flow cytometry and cell sorting in immunological studies (second edition). *Eur J Immunol* **49**, 1457-1973, doi:10.1002/eji.201970107 (2019).
39 Heinen, A. P. *et al.* Improved method to retain cytosolic reporter protein fluorescence while staining for nuclear proteins. *Cytometry A* **85**, 621-627, doi:10.1002/cyto.a.22451 (2014).
40 Hsiau, T. *et al.* Inference of CRISPR edits from Sanger trace data. *BioRxiv*, doi:10.1101/251082 (2019).
41 Zheng, G. X. *et al.* Massively parallel digital transcriptional profiling of single cells. *Nat Commun* **8**, 14049, doi:10.1038/ncomms14049 (2017).
42 Stuart, T. *et al.* Comprehensive Integration of Single-Cell Data. *Cell* **177**, 1888-1902.e1821, doi:10.1016/j.cell.2019.05.031 (2019).
43 Kim, D., Langmead, B. & Salzberg, S. L. HISAT: a fast spliced aligner with low memory requirements. *Nat Methods* **12**, 357-360, doi:10.1038/nmeth.3317 (2015).
44 Anders, S., Pyl, P. T. & Huber, W. HTSeq--a Python framework to work with high-throughput sequencing data. *Bioinformatics* **31**, 166-169, doi:10.1093/bioinformatics/btu638 (2015).
45 Henikoff, S., Henikoff, J. G., Kaya-Okur, H. S. & Ahmad, K. Efficient chromatin accessibility mapping in situ by nucleosome-tethered tagmentation. *Elife* **9**, doi:10.7554/eLife.63274 (2020).
46 Love, M. I., Huber, W. & Anders, S. Moderated estimation of fold change and dispersion for RNA-seq data with DESeq2. *Genome Biol* **15**, 550, doi:10.1186/s13059-014-0550-8 (2014).
47 Langmead, B. & Salzberg, S. L. Fast gapped-read alignment with

Bowtie 2. *Nat Methods* **9**, 357-359, doi:10.1038/nmeth.1923 (2012).
48 Ramírez, F. *et al.* deepTools2: a next generation web server for deep-sequencing data analysis. *Nucleic Acids Res* **44**, W160-165, doi:10.1093/nar/gkw257 (2016).
49 Zhang, Y. *et al.* Model-based analysis of ChIP-Seq (MACS). *Genome Biol* **9**, R137, doi:10.1186/gb-2008-9-9-r137 (2008).

Acknowledgments

This study was supported by grants from National Natural Science Foundation of China (31630021, 31930037, 82071843 and 81901637), National Human Genetic Resources Sharing Service Platform (2005DKA21300), Shanghai Municipal Key Medical Center Construction Project (2017ZZ01024-002), Shenzhen Science and Technology Project (JCYJ20180504170414637 and JCYJ20180302145033769), Shenzhen Futian Public Welfare Scientific Research Project (FTWS2018005), and Sanming Project of Medicine in Shenzhen (SZSM201602087).

Author contributions

Conceptualization: N.S., D.D., C.G.V.; Methodology: D.D., S.G.; Formal analysis: D.D.; Experiment conduction: S.G., D.D., X.H., J.Z., G.H., B.Q., H.Z.; Resources: H.D., Q.G., S.C., Z.Y., J.Q., Z,Y., N.S.; Bioinfomatic analysis: C.Y., D.D.; Writing - Original Draft: D.D.; Writing - Review & Editing: C.G.V., D.D., N.S.; Supervision: N.S., D.D.; Funding acquisition: N.S.

Data availability

The sc-RNAseq, RNAseq and cut-tag sequencing data have been deposited in ArrayExpress database and the accession code will be provided prior to publication. Source data are available upon request.

Competing Interests

The authors declare no competing interests.

Additional information

Methods
Extended Data Figs. 1 to 9
Figure legends for Extended Data Figs. 1 to 9
Supplementary Tables 1-6

484 **Methods**

485 **Mice and Bm12 cGVHD lupus models.**

486 The C57BL/6J (JAX000664), Bm12 (JAX001162), Cd19-Cre (JAX006785), B6
487 Cd45.1(JAX002014) and Cas9-EGFP (JAX026175) mice were obtained from
488 Jackson Laboratory. Zeb2^{flox} mice (T015122) were obtained from
489 Gempharmatech (Nanjing). All the mouse strains were on C57BL/6 background
490 and maintained under specific pathogen free (SPF) conditions in Renji Hospital
491 animal facilities. All procedures involving animals were approved by Institutional
492 Animal Care and Use Committee at Renji Hospital of Shanghai Jiaotong
493 University School of Medicine (SJTUSM).

494

495 Bm12-cGVHD lupus model was induced following JOVE protocol[37]. Briefly, 8-
496 12-week-old mice were intraperitoneally injected with 10 million CD4^{+} T cells
497 (Miltenyi Biotec, Cat#130-104-454) from Bm12 mice purified by magnetic cell
498 sorting and mice were sacrificed for analysis at indicated time points. For Jak-
499 Stat inhibitor treatment experiment, mice were orally gavage with 30 mg/kg
500 tofacitinib (Selleckchem, Cat#S2789) for 2 weeks.

501

502 **Patients subject**

503 All patients were recruited from Renji Hospital. SLE patients met American
504 College of Rheumatology criteria for SLE. Demographic and clinical information
505 is listed (Supplementary Table 1 for scRNAseq, Supplementary Table 2 for
506 detection of *ZEB2* and *IL-21R*). RA patients met the 2010 American College of
507 Rheumatology criteria for RA. Clinical and laboratory data of RA patients were
508 measured at baseline and at week 4 after tofacitinib treatment. Demographic
509 and clinical information is listed before and after treatment (Supplementary
510 Table 3). All procedures were fully consent under ethical and safe protocols
511 approved by the Review Board at Renji Hospital of SJTUSM.

512

513 **Cell isolation, flow cytometry and sorting.**

514 Single cell suspensions of splenocytes were subjected to red blood cell lysis
515 and filtered through 70 um nylon mesh. Cells were stained for surface markers
516 or intracellular proteins under instructions[38]. For in vitro differentiation
517 experiment, B cells transfected sgRNA plasmids (BFP) were stained with
518 surface markers and then fixed by 2% fresh prepared formaldehyde in PBS for
519 5 minutes to allow efficient TF and cytokine staining and retain FP which were
520 optimized from previous protocol[39]. For intracellular T-bet staining, cells were
521 fixed and permeabilized after surface staining using Foxp3 Transcription Factor
522 Staining Buffer Set (ThermoFisher, Cat#00-5523-00). Samples were acquired
523 using LSRFortessa (BD Biosciences) and analyzed using FlowJo software
524 (Tree Star) .
525
526 For sorting experiment, splenic B cells were enriched by magnetic microparticle
527 purification using mouse B Cell Isolation Kit (Miltenyi Biotec, Cat#130-090-862)
528 and then further sorted by gating $CD11c^+$ B cells ($CD19^+CD11c^+CD21^-$) and
529 $CD11c^-$ B cells ($CD19^+CD11c^-CD21^+$) using FACSAria II (BD Biosciences).
530 Detailed information of antibodies were listed in Supplementary Table 4
531
532 **In vitro induction of ABC and ASC.**
533 Mouse splenic B cells were purified by negative selection and cultured in RPMI-
534 1640 medium with 10% fetal bovine serum, HEPES, non-essential amino acids
535 (NEAA), glutamine, sodium pyruvate, β-Mercaptoethanol and
536 penicillin/streptomycin. ABCs were induced in the presence of R848 (500 ng/ml,
537 Invivogen, Cat#tlrl-r848-5), anti-CD40 (1 ug/ml, Biolegend, Cat#102812), anti-
538 IgM $F(ab')_2$ (1 ug/ml, Jackson Immunoresearch, Cat#115-006-020), IL-21 (50
539 ng/ml, Peprotech, Cat#210-21), IFN-γ (1, 5 or 10ng/ml, Biotech, Cat#485-MI-
540 100) for 3 days. A similar procedure was done by replacing IFN-γ with IL-4 (10
541 ng/ml, Peprotech, Cat#214-14). To induce ASCs, B cells derived above were
542 transferred into new well and cultured for additional 4 days with indicated
543 stimulation cocktails.

544

545 Human PBMCs were isolated by density gradient centrifugation using Ficoll-
546 Paque (GE Healthcare, Cat#17-5442-03). B cells were purified by negative
547 selection (Miltenyi Biotec, Cat#130-091-151) from PBMCs and stimulated with
548 R848 (1 ug/ml), CD40L (10 ug/ml, Biolegend, Cat#591708), BAFF (20 ng/ml,
549 Peprotech, Cat#310-13-20), IL-2 (10 ng/ml, Peprotech, Cat#200-02), Goat
550 Anti-Human IgA + IgG + IgM (H+L) (10 ug/ml, Jackson Immunoresearch,
551 Cat#109-006-064), IL-21 (10 ng/ml, Biolegend, Cat#571204), IFN-γ (20 ng/ml,
552 Biolegend, Cat#570206) for 3 days and stained with anti-human CD19, CD38,
553 CD27, IgD, CD11c, CD21, T-bet to detect ABC formation. Addition of Tofacitinib
554 and Baricitinib (Selleckchem, Cat#S2851) were indicated.

555

556 **Vector construction, sgRNA cloning, retrovirus packaging and infection.**
557 For the transcription factor screening, sgRNA designed by online design tool
558 (http://chopchop.cbu.uib.no/) and two DNA oligo annealing by T4
559 Polynucleotide Kinase (NEB, Cat#M0201L) and cloned into a Bbs1-digested
560 U6-sgRNA-PGK-Puro-BFP retrovirus vector by T4 DNA ligation. The day before
561 transfection, 80 million Plate-E cells were plated in 10 cm dish in DMEM with
562 10% FBS. Cells were transfected with 15 ug sgRNA plasmid using 30 μL of
563 Lipofectamine 2000 (Invitrogen, Cat#11668019). Plat-E cells were further
564 cultured for 48 hours. The retrovirus supernatants were centrifuged and debris
565 were removed. Retrovirus were spin transduced to activated B cells in the
566 presence of polybrene (10 ug/ml, Sigma, Cat#H9268) with 1260 RCF for 90
567 minutes at temperature of 32℃. The medium was removed six hours later and
568 replaced with fresh medium for ABC induction. At least 4 single guide RNA
569 (sgRNA) plasmids (co expressing blue fluorescent protein, BFP as reporter)
570 were constructed per gene target and validated editing efficiency in mouse
571 primary B cells using the online ICE tool (Inference of CRISPR Edits;
572 Synthego)[40]. We select the most efficient sgRNA with an editing rate over 50%

573 for further functional screening. The selected sgRNA sequences were listed in
574 Supplementary Table 5.
575
576 **Human B cell editing.**
577 Purified B cells from human PBMC were stimulated with R848(1ug/ml), IL-
578 2(10ng/ml), BAFF (20ng/ml), Goat Anti-Human IgA/IgG /IgM (H+L) (10ug/ml)
579 for one day. The next day, synthetic sgRNA oligos (GenScripts) were co-
580 incubated with Cas9 protein (GenScripts, Cat#Z03389) at room temperature for
581 20 minutes. 0.1 million cells were washed and electroporated using the Neon
582 transfection system (Thermofisher, Cat#MPK5000S) following manufacturer's
583 instruction. For candidate TFs, we selected sgRNAs with editing efficiency over
584 50%. The selected sgRNA sequences were listed in Supplementary Table 5.
585 After electronical transfection, human B cells were induced to ABC
586 differentiation described above.
587
588 **Antibody titers.**
589 Serum samples were collected at indicated time points to detect anti-dsDNA by
590 ELISA (Alpha Diagnostic International, Cat#5110) and Hep-2 cells slides (Inova
591 diagnostics Cat#708750) were used to detect anti-nuclear antibodies. FITC-
592 anti-mouse IgG were used as detection antibody for ANA. Antibody from culture
593 supernatant was diluted and captured by goat anti-mouse Ig (Southern
594 Biotechnology, Cat#5300-05B) and detected by HRP- labeled goat anti-mouse
595 IgG1, IgG2c, IgG3 or IgM specific Abs and TMB substrate (Biotech, Cat#DY999)
596 followed by sulfuric acid stop. Absorbance values at 370/450 nm (OD) were
597 read and absolute titers were calculated from standard curves, which were
598 generated from purified mouse Ig isotype (Southern Biotechnology, Cat#5300-
599 01B).
600
601 **RNA extraction and quantitative RT-PCR analysis.**
602 Total RNA was extracted from B cells with TRIzol reagent (ThermoFisher,

603 Cat#15596026) according to the manufacturer's instructions. RNA quantity and
604 quality were assessed using the Nanodrop 2000. cDNA was synthesized using
605 PrimeScript™ RT Reagent Kit (TaKaRa, Cat#RR037A) , Real-time PCR
606 reactions were performed using TB Green Premix Ex Taq reagent (TaKaRa,
607 Cat#RR420A) on QuantStudio 7 Flex (Applied Biosystems). For quantification
608 of gene expression, each sample was normalized to expression of an
609 endogenous control gene Rpl13a. All primers used were listed in
610 Supplementary Table 6.
611

612 **Single-cell RNA library preparation and sequencing**

613 After FACS sorting of $ZA^{-}CD19^{+}$ B cells from PBMC of patient with new-onset
614 SLE, 12000 cells were counted and viability was confirmed to be >90%. Single-
615 cell suspensions were loaded on a 10X Genomics Chromium single-cell 5′ v2
616 chip to prepare the libraries according to the manufacturer's protocol. The
617 library quality was checked by Agilent 2100 Bioanalyzer and Qubit fluorometric
618 quantitation. Samples were sequenced on an Illumina NovaSeq 6000 with a
619 sequencing depth of at least 50k reads per cell.
620

621 **Processing of single-cell RNA-seq data**

622 The raw FASTQ data were processed with Cell Ranger (v3.1.1) [41] by using
623 GRCm38 annotation (v1.2.0). Output from Cell Ranger was loaded into R and
624 used Seurat (v3.1.1) [42] package for further analysis. Total 5721 cells with fewer
625 than 500 or more than 5000 expressed genes, a high percentage of
626 mitochondrial genes (>10%) were removed. Next, the UMI counts in each cell
627 were normalized and scaled. The top 1500 highly variable genes were used for
628 dimensionality reduction using Principal Components Analysis. Upon 'Elbow
629 plot', we selected the first 15 PC for clustering and UMAP visualization with
630 default parameters. For clustering, we first selected resolution parameter = 0.8
631 which produced 9 clusters. To obtain cluster-specific gene signatures, we
632 identified differential expression analysis of each cluster against the others

633 using wilcox with parameter (logfc. threshold = 0.25, min.pct=0.1). Clusters
634 were manually merged with the nearest cluster based on the phylogenetic tree
635 from Seurat's Build Cluster Tree and similar marker genes. Finally, we got 7
636 clusters for downstream analysis.
637
638 **RNAseq.**
639 Cas9-EGFP mouse B cells were retrovirally transduced with sg-NC, sg-Zeb2,
640 sg-T-bet plasmids after activation for 1 day and further cultured under in vitro
641 ABC induction condition for 72 hours. Cells were stained withanti-mouse CD19
642 and $CD19^{+}EGFP^{+}BV421^{+}$ cells were sorted. Sorted cells were washed twice
643 and resuspended in TRIzol reagent. Total RNA was extracted and used as input
644 for Illumina TruSeq RNAseq library kit. After quality assessment, RNAseq
645 libraries were pooled. 50 bp paired-end sequencing was performed using
646 Illumina HiSeq2000.
647
648 Clean reads were aligned to mm10 reference genome with Hisat2 (v2.1.0) [43]
649 using default parameters. Gene expression levels were counted with HT-
650 seq(v0.11.2) [44] [45]using default 'union' mode. Differential expressions of genes
651 were conducted by DESeq2(v1.24.0) package [46] and simple plots were
652 produced in R(v3.3.3). GSEA was performed using the online software (Broad
653 Institute) (http://software.broadinstitute.org/gsea/index.jsp).
654
655 **CUT-Tag**
656 CUT&Tag libraries were generated following instructions described previously[34]
657 and manufacturer's protocol (Vazyme, Cat#TD901-01). Briefly, 0.5 million in
658 vitro derived mouse ABCs were incubated with CoA-coated magnetic beads,
659 and then primary antibodies (anti-Zeb2 and anti-Tbet) were added to incubate
660 for 1 hours at room temperature. After incubation, secondary antibodies
661 (incubated at RT for 1 hours) and pG-Tn5 adapter complex (incubated at RT for
662 1 hours) were added. Then, tagmentation took place for 1 hours, and DNAs

were extracted using phenol–chloroform–isoamyl alcohol. Libraries were prepared and cleaned up using Ampure XP beads (Beckman Coulter) and pooled together for paired-end sequencing.

Sequencing data were analyzed as follows. After trimming the adapters of reads and removing low-quality bases by TrimGalore software in paired-end mode, clean reads were mapped to mm10 reference genome with Bowtie2 (v2.3.5) [47] followed by removing PCR duplicates using Picard (v2.19.0).The genome browser tracks in bigwig format were produced from merged replicates using deepTools (v2.0) [48] and peaks were called using MACS2 (v2.1.2) [49] using parameters '-f BAMPE –SPMR -nomodel'. Enriched transcription factor binding motifs were searched by HOMER (v4.11). A set of sequences were searched for individual matches to each of the motif using FIMO (https://meme-suite.org/meme/tools/fimo). All analysis data were visualized using the IGV software(Broad Institute).

Statistical analysis

Prism software (GraphPad) was used for statistical analyses. Data were shown as mean ± SEM values. All data points represented the measurement of distinct samples. Differences were evaluated by analysis of variance followed by unpaired two-tailed Student's *t* test with 95% confidence intervals to compare between two normally distributed groups with equal variances unless specified. Spearman's test was adopted to carry out the correlation analysis. P values of less than 0.05 were considered significant.

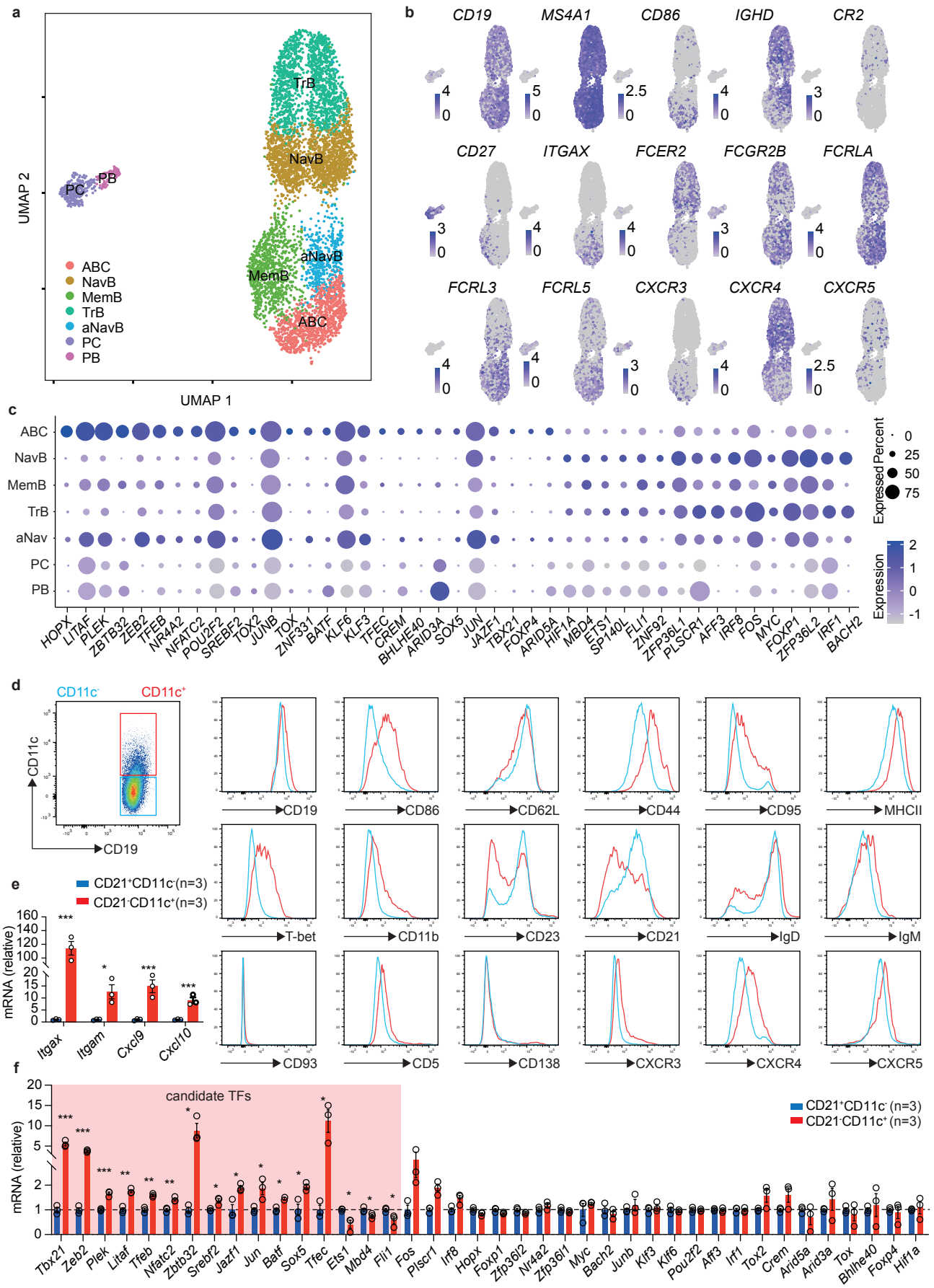

Fig 1. Identification of differentially-expressed transcriptional factors in ABCs.
(**a**) CD19⁺ B cells were sorted from PBMCs of new-onset SLE patient and performed droplet-based scRNA-seq. Unsupervised clustering was visualized with two dimensional UMAP. Seven clusters are defined and annotated as transitional B cells (TrB), naïve B cells (NavB), activate naïve B cells (aNavB), ABC, memory B cells (MemB), plasma blasts (PB) and plasma cells (PC). Each point is a single cell colored by cluster assessment. (**b**) UMAP plots of selected genes expressions to distinguish ABCs. Color scales for each gene show log-normalized expression levels. (**c**) Dot plots of 43 differentially-expressed transcription factors in ABCs with 27 upregulated TFs and 16 downregulated TFs. Dot size represents proportion of cells expressing indicated TF in particular cluster and intensity of color represents the average expression level. (**d**) C57/B6 mice were intraperitoneally injected with 10 million CD4⁺ T cells from Bm12 mice for 2 weeks and sacrificed for detection. Flow cytometry detection of splenic CD11c⁻ (blue) or CD11c⁺ (red) B cells (n=3) for ABC specific markers. (**e-f**) QPCR analysis of ABC signature genes (*Itgam*, *Itgax*, *Cxcl9*, *Cxcl10*) and mouse genes encoding equivalent TFs which identified in **c** from splenic CD11c⁻ (blue) or CD11c⁺ (red) B cells (n=3) sorted by flow cytometry at week 2 after Bm12 induction described in **d**. n refers to the measurement of distinct samples (biological repeats). Data are representative of two in **d** and three in **e**,**f** independent experiments with 3 mice per group. Bars indicate mean ± SEM values. Statistical significance determined by Student's t test.*p < 0.05, **P < 0.01, ***P < 0.001, ns, not significant.

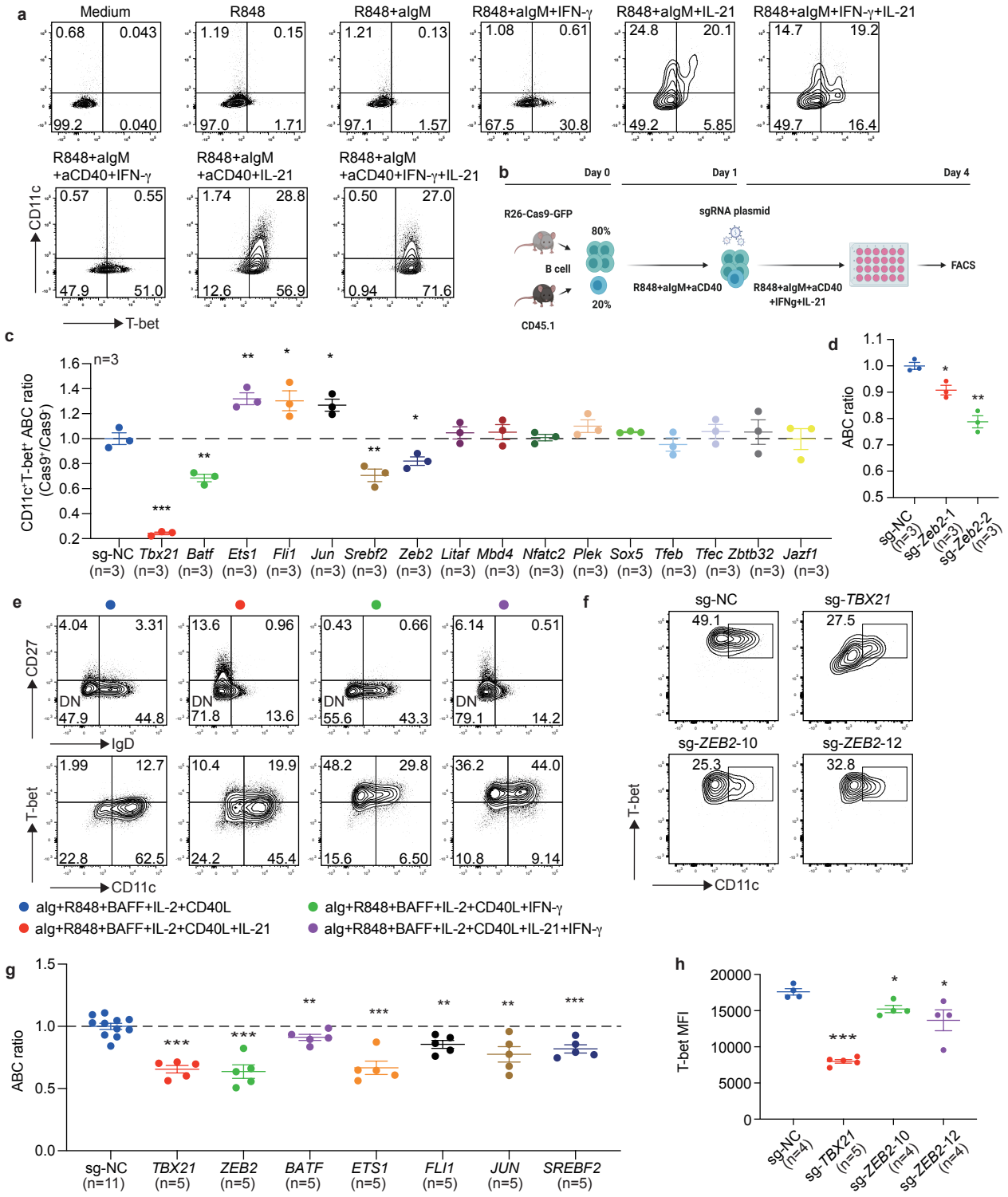

Fig 2. Cas9 based screen of transcription factors for ABC differentiation.
(**a**) Flow cytometry plots of mouse ABCs (CD11c$^+$T-bet$^+$) derived from in vitro induction. (**b**) Flow chart of Cas9 based screen and in vitro mouse ABC differentiation assay. On day 0 (D0), splenic B cells from Cas9-EGFP and B6 CD45.1 mouse were mixed at a ratio of 4:1 and activated by anti-IgM, anti-CD40 and R848. On day 1(D1), activated B cells were retroviral infected with sgRNA-plasmids and further cultured with the ABC differentiation cocktail for 3 days. On day 4 (D4) cells were stained with surface markers and fixed/permed for fluorescent protein and intracellular T-bet detection. (**c**) Statistical analysis of ABC (CD11c$^+$T-bet$^+$) ratio in groups targeting indicated genes. ABC ratio was caculated as in **Extended Data Fig. 3a**. (**d**) Statistical analysis of ABC (CD11c$^+$T-bet$^+$) ratio in retroviral infected B cells of two distinct sgRNAs targeting *Zeb2*. (**e**) Flow cytometry plots of human DN (CD27$^-$IgD$^-$) and ABCs (CD27$^-$IgD$^-$CD11c$^+$T-bet$^+$) derived from in vitro induction. (**f-g**) Human B cells were activated and electroporated with Cas9-RNP targeting indicated genes and then cultures with the human ABC differentiation cocktail (anti-Ig, R848, CD40L, Baff, IL-2, IFN-γ and IL-21) for a further 3 days. Flow cytometry plots (**f**) and statistical analysis (**g**) of human ABCs (CD27$^-$IgD$^-$CD11c$^+$T-bet$^+$) after gene editing and in vitro differentiation. ABC ratio was normalized with sg-NC. (**i**) Statistical analysis of T-bet MFI in sg-*TBX21* and two distinct sg-*ZEB2* edited human B cells, comparing with sg-NC. n refers to the measurement of distinct samples (biological repeats). Data are representative of 3-4 independent experiments. Bars indicate mean ± SEM values. Statistical significance determined by Student's t test.*p < 0.05, **P < 0.01, ***P < 0.001, ns, not significant.

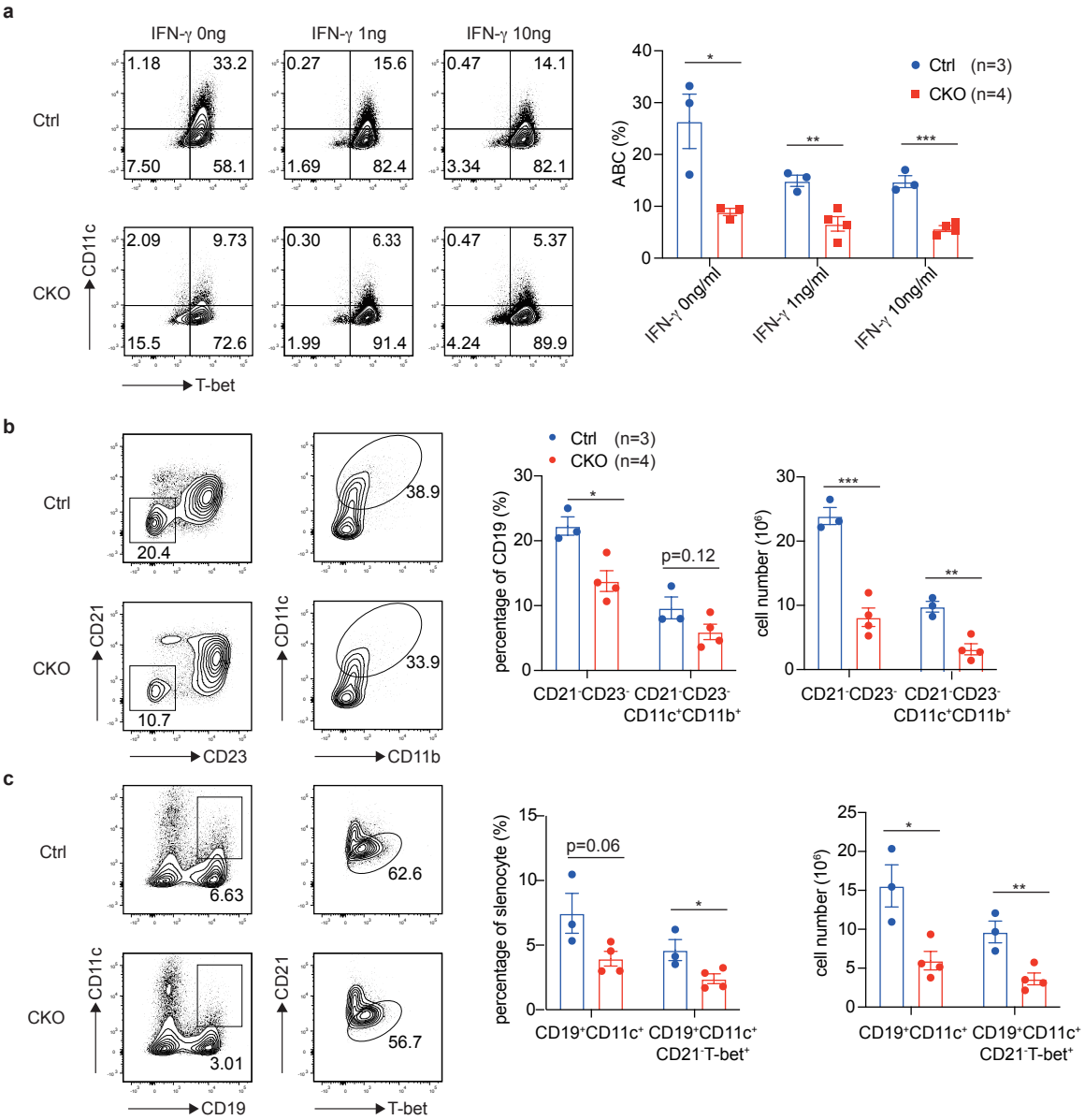

Fig 3. Zeb2 drives ABC differentiation.
(**a**) Splenic B cells were isolated from Zeb2$^{flox/flox}$ CD19$^{+/+}$(Ctrl) and Zeb2$^{flox/flox}$ CD19$^{Cre/+}$(CKO) mice and cultured with cocktail (anti-IgM, R848, anti-CD40 and IL-21) and different IFN-γ concentration for 3 days. Flow cytometry plots (left) and statistical analysis (right) of ABCs (CD11c^{+}T-bet^{+}). (**b-c**) Zeb2$^{flox/flox}$ CD19$^{+/+}$(Ctrl) and Zeb2$^{flox/flox}$ CD19$^{Cre/+}$(CKO) mice were intraperitoneally injected with 10 million CD4^{+} T cells of Bm12 mice for 2 weeks. Flow cytometry plots (left) and statistical analysis (right) by different staining panels related to ABC characters. CD19^{+}CD21^{-}CD23^{-} and CD19^{+}CD21^{-}CD23^{-}CD11c^{+}CD11b^{+} were analyzed as in **b**. CD19^{+}CD11c^{+} and CD19^{+}CD11c^{+}CD21^{-}T-bet^{+} were analyzed in **c**. n refers to the measurement of distinct samples (biological repeats). Data are representative of 2 independent experiments. Bars indicate mean ± SEM values. Statistical significance determined by Student's t test.*$p < 0.05$, **$P < 0.01$, ***$P < 0.001$, ns, not significant.

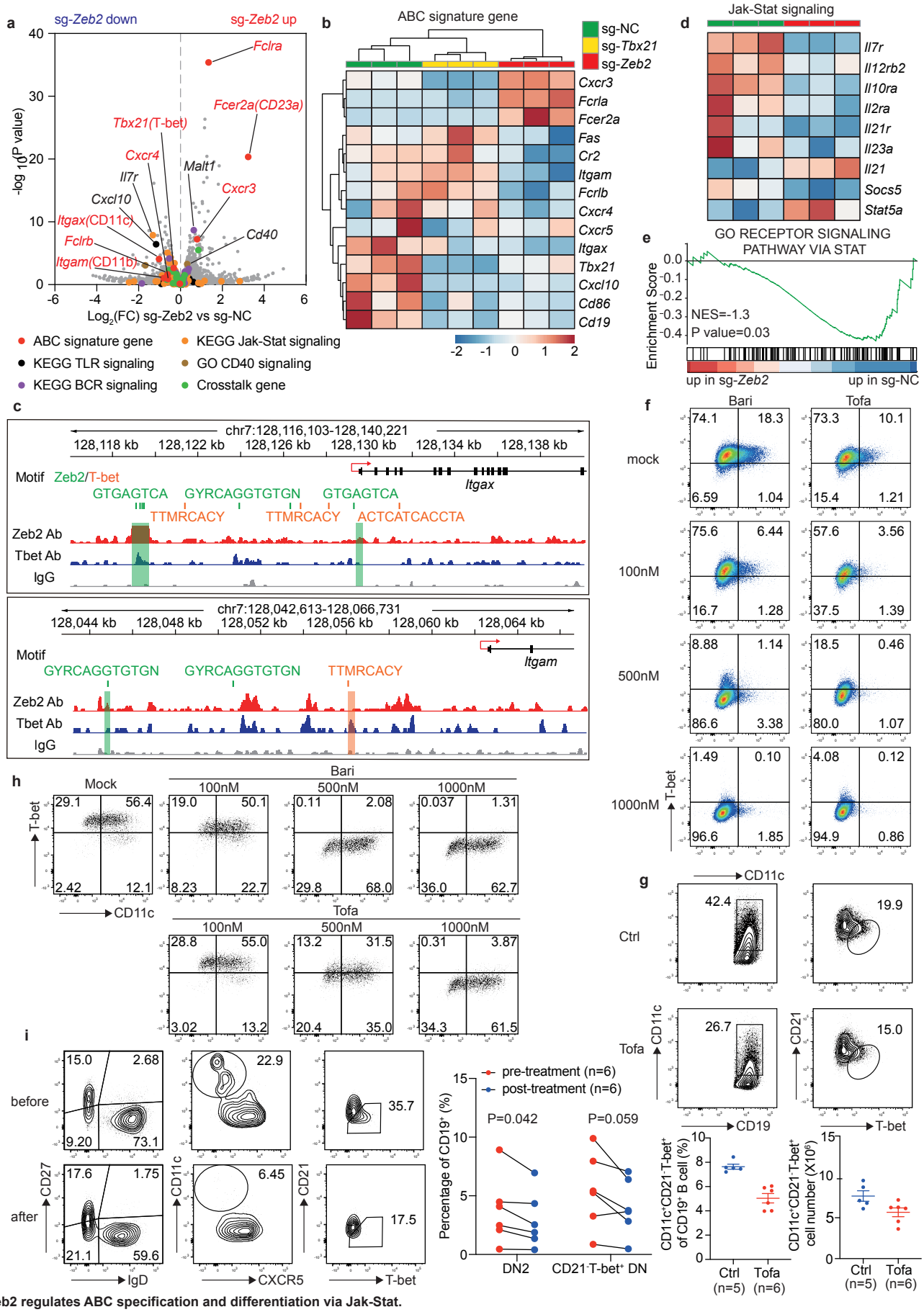

Fig. 4 Zeb2 regulates ABC specification and differentiation via Jak-Stat.

(a) Volcano graph showing the transcriptional profiles in mouse B cells edited by sg-NC and sg-*Zeb2* with the ABC induction cocktail for 3 days. ABC signature genes, genes of BCR, TLR, Jak-Stat signaling from KEGG database, GO CD40 signaling and crosstalk genes were labeled with colored dots. (**b**) Heatmap showing expression of representative ABC signature genes in mouse B cells edited by sg-NC, sg-*Zeb2*, sg-*Tbx21*. Genes and groups were clustered. (**c**) IGV trunk view of open chromatin region (OCR) signals in transcriptional regulatory sites of *Itgax* and *Itgam*. IgG (gray line), Zeb2 (red line) and T-bet (blue line) specific signals at indicated loci were shown. Consensus Zeb2 (green) and T-bet (orange) binding motifs within the differentially accessible regions were indicated. (**d**) Heatmap showing expression of selected Jak-Stat signaling genes in sg-NC$^+$ and sg-Zeb2$^+$ B cells. (**e**) GSEA showing impaired receptor signaling pathway via Stat in sg-Zeb2$^+$ B cells compared with sg-NC. (**f**) Flow cytometry plots of in vitro induced mouse ABCs (CD11c$^+$T-bet$^+$) with different concentration of baricitinib (Bari) or tofacitinib (Tofa). (**g**) C57 mice were intraperitoneally injected with 10 million CD4$^+$ T cells of Bm12 mice for 2 weeks and treated with tofacitinib (Tofa) or disolved solution (Ctrl) by oral gavage once a day. Flow cytometry plots and statistical analysis of splenic ABCs (CD19$^+$CD11C$^+$T-bet$^+$CD21$^-$). (**h**) Flow cytometry plots of in vitro induced human ABCs (CD11c$^+$T-bet$^+$) with different concentration of baricitinib or tofacitinib. (**i**) Flow cytometry plots of human ABCs (DN2, CD19$^+$CD27$^-$IgD$^-$CD11c$^+$CXCR5$^-$) or (CD21$^-$T-bet$^+$ DN, CD19$^+$CD27$^-$IgD$^-$CD21$^-$T-bet$^+$) in PBMCs from patients with rheumatoid arthritis before and after Jak-Stat inhibitor tofacitinib treatment for 4 weeks. n refers to the measurement of distinct samples (biological repeats). Data are representative of 3 independent experiments in f-h. Bars indicate mean ± SEM values. Statistical significance determined by Student's t test.*$p < 0.05$, **$P < 0.01$, ***$P < 0.001$, ns, not significant.

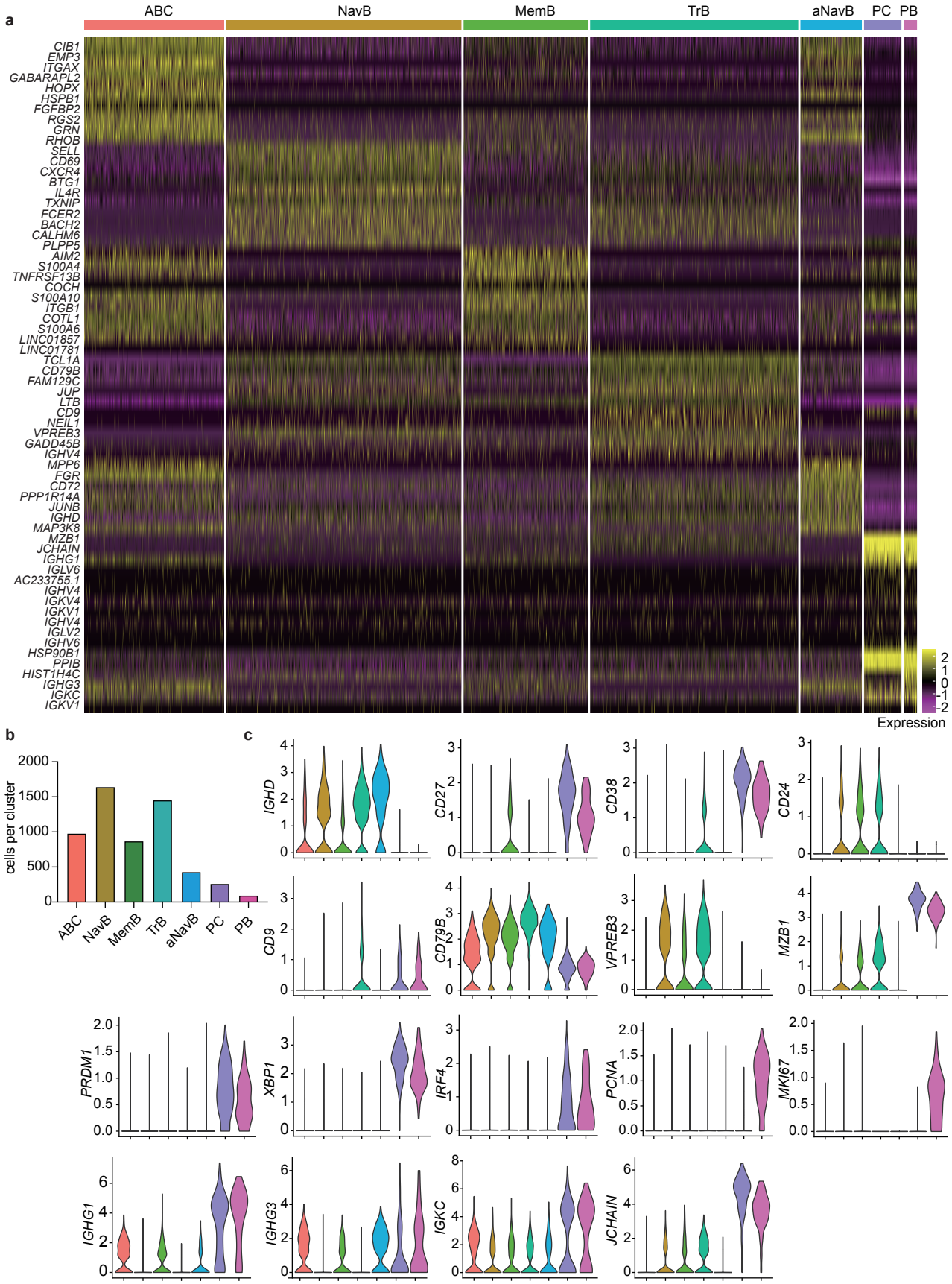

Extended Data Fig. 1 B cells landscape of a new-onset SLE patient.
(**a**) Heat map representing scaled expression values of top 10 genes defining each cluster. (**b**) Number of cells per cluster. (**c**) Violin plots of selected gene expression (*IGHD, CD27, CD38, CD24, CD9, CD79B, VPREB3, MZB1, PRDM1, XBP1, IRF4, PCNA, MKI67, IGHG1, IGHG3, IGKC, JCHAIN*) in different clusters, with log-normalized expression values labeled.

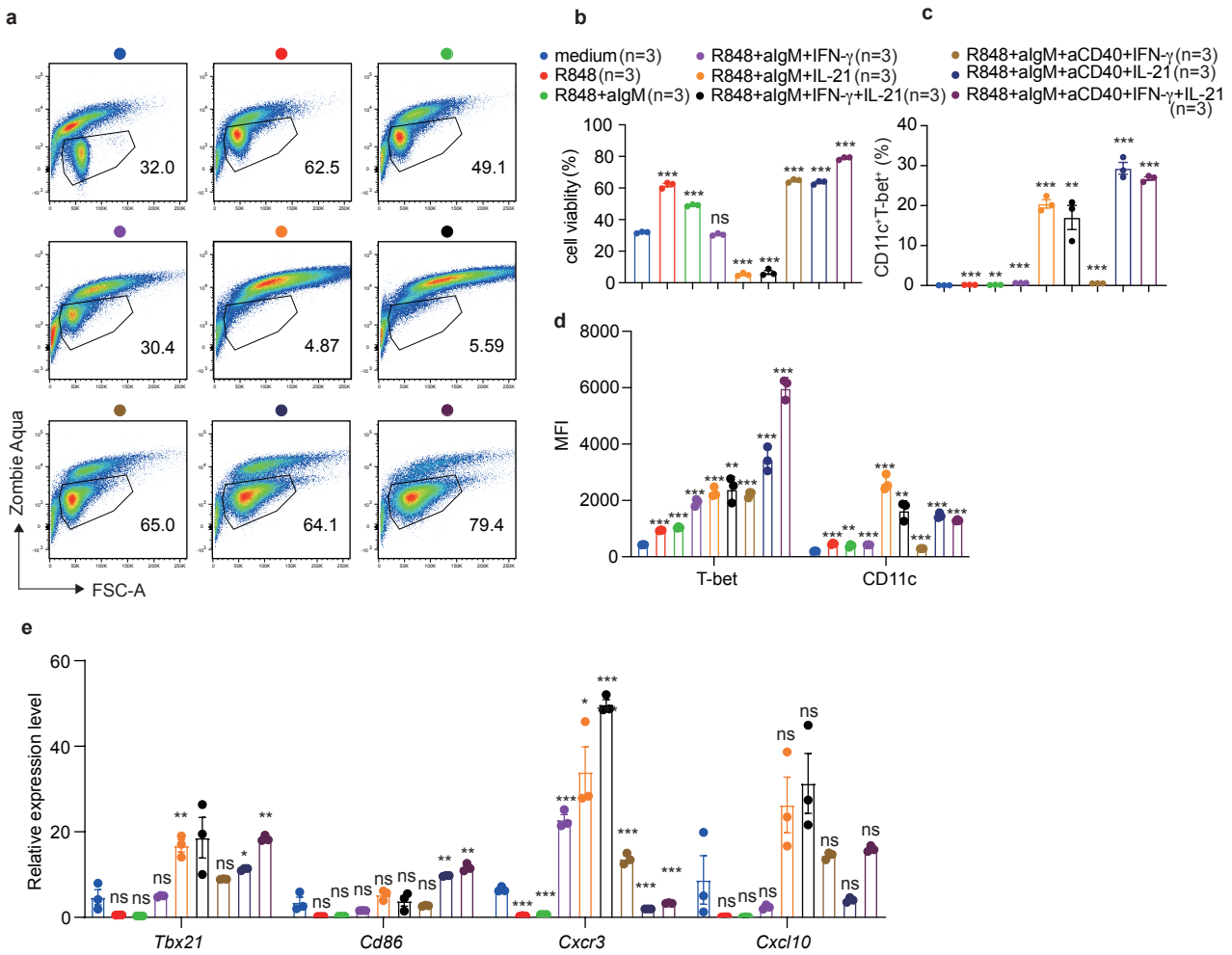

Extended Data Fig. 2 In vitro induction of mouse ABCs.
(**a-b**) Flow cytometry plots (**a**) and statistical analysis (**b**) of viability from B cells cultured with indicated cocktail for 3 days described as in **Fig. 2a**. (**c**) Statistical analysis of mouse ABCs (CD11c$^+$T-bet$^+$) from in vitro induction described as in **Fig. 2a**. (**d**) MFIs of T-bet and CD11c of B cells described as in **Fig. 2a**. (**e**) QPCR analysis of *Tbx21*, *Cd86*, *Cxcr3* and *Cxcl10* expression from in vitro induced B cells described as in **Fig. 2a**. n refers to the measurement of distinct samples (biological repeats). Data are representative of 3 independent experiments. Bars indicate mean ± SEM values. Statistical significance determined by Student's t test.*$p < 0.05$, **$P < 0.01$, ***$P < 0.001$, ns, not significant.

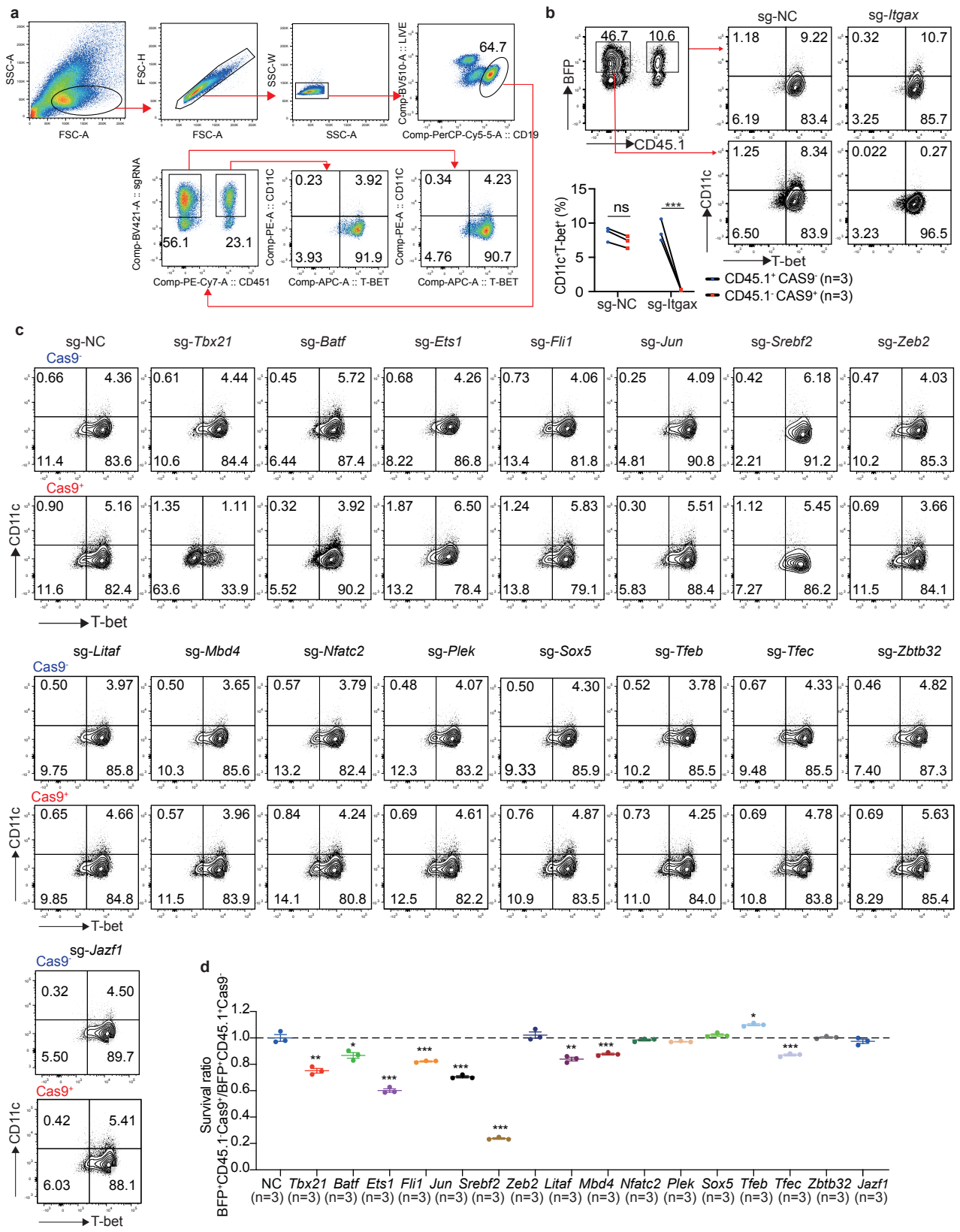

Extended Data Fig. 3 Gene editing in mouse primary B cells and screen TFs for ABC differentiation.
(**a**) Splenic B cell were activated, retroviral infected and induced for ABC differentiation described as in **Fig. 2b**. Gating strategy for flow cytometry analysis. Cells with certain size gated by FSC-A and SSC-A following duplicates exclusion by FSC-A/H and SSC-A/W. Then viable B cells were gated from CD19$^+$Zombie Aqua$^-$ and further divided into BFP$^+$CD45.1$^-$ fraction and BFP$^+$CD45.1$^+$ fraction. ABC frequencies were gated with CD11c$^+$T-bet$^+$. Then ABC frequency were compared between BFP$^+$CD45.1$^-$ fraction and BFP$^+$CD45.1$^+$ fraction and caculated as ABC rates. ABC rates in sg-TF group normalized with sg-NC group were set as ABC ratio. (**b**) Flow cytometry plots and frequency of ABCs (CD11c$^+$T-bet$^+$) in CD45$^+$sg-*Itgax*$^+$ (Cas9$^-$) and CD45.1$^-$sg-*Itgax*$^+$ (Cas9$^+$) cells described as in **a**. (**c**) Flow cytometry plots of ABCs (CD11c$^+$T-bet$^+$) in CD45$^+$sgRNA$^+$ (Cas9$^-$sgRNA$^+$) and CD45.1$^-$sgRNA$^+$ (Cas9$^+$sgRNA$^+$) cells targeting indicated genes. (**d**) Statistical analysis of cell survival ratio by comparing CD45.1$^-$(GFP$^+$) with CD45.1$^+$(GFP$^-$) B cells and then normalized with sg-NC. n refers to the measurement of distinct samples (biological repeats). Data are representative of 4 independent experiments. Bars indicate mean ± SEM values. Statistical significance determined by Student's t test.*p < 0.05, **P < 0.01, ***P < 0.001, ns, not significant.

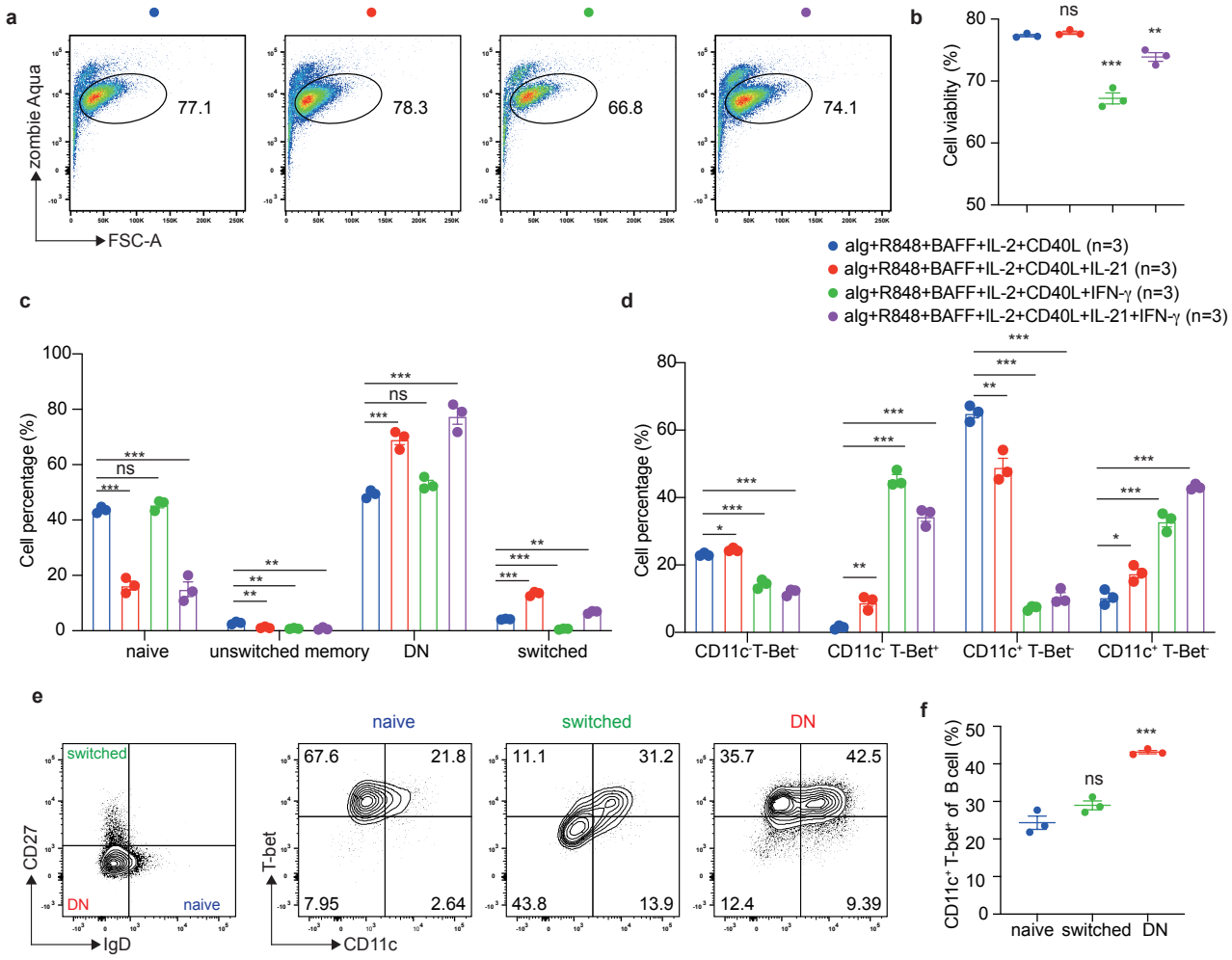

Extended Data Fig. 4 In vitro induction of human ABCs.
(**a-b**) Flow cytometry plots (**a**) and statistical analysis (**b**) of viability of B cells cultured in indicated cocktail described as in **Fig. 2f**. (**c**) Statistical analysis of naïve ($CD19^+CD27^-IgD^+$), DN ($CD19^+CD27^-IgD^-$), switched memory ($CD19^+CD27^+CD38^-IgD^-$) and unswitched memory ($CD19^+CD27^+IgD^+$) B cells generated from B cells cultured in indicated cocktail described as in **Fig. 2f**. (**d**) Frequencies and statistical analysis of $CD11c^+T\text{-}bet^-$, $CD11c^-T\text{-}bet^+$, $CD11c^-T\text{-}bet^-$ and $CD11c^+T\text{-}bet^+$ B cells from in vitro induction described as in **Fig. 2f**. (**e-f**) Flow cytometry plots (**e**) and statistical analysis (**f**) of $CD11c^+T\text{-}bet^+$ B cells in DN, naïve, switched memory B cells generated from B cells cultured with the human ABC induction cocktail for 3 days. n refers to the measurement of distinct samples (biological repeats). Data are representative of 2 independent experiments. Bars indicate mean ± SEM values. Statistical significance determined by Student's t test.*$p < 0.05$, **$P < 0.01$, ***$P < 0.001$, ns, not significant.

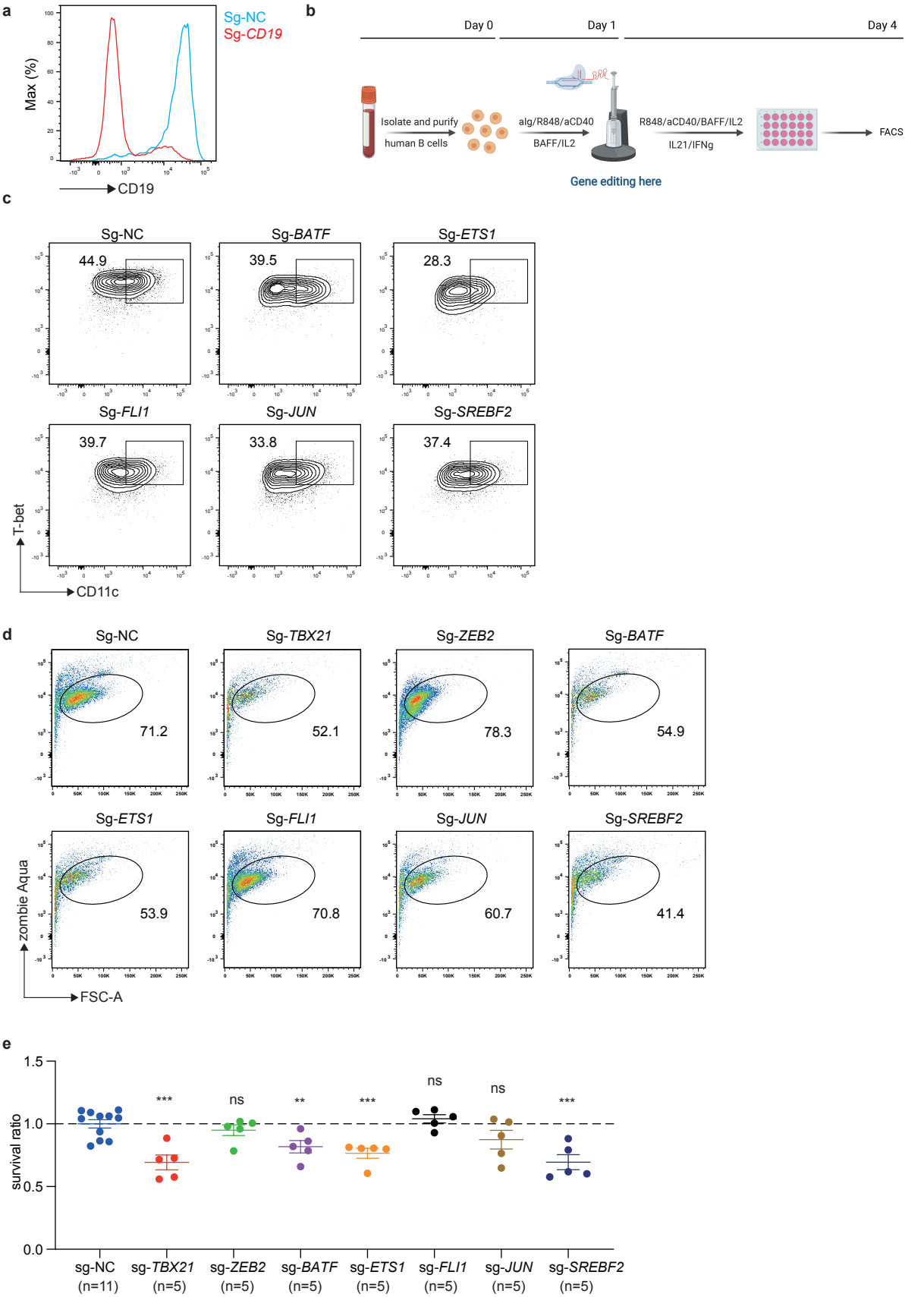

Extended Data Fig. 5 Screen TFs for human ABC differentiation.
(**a**) Cas9 RNP delivery to primary B cells. Positive control sg-*CD19* was used to verify efficiency of gene editing in human primary B cells. (**b**) Flow chart of Cas9-RNP based screen and in vitro human ABC differentiation assay. On day 0, human B cells were activated by anti-Ig, R848, CD40L, BAFF, IL-2. On day 1, activated B cells was electronical delivered of Cas9-RNP and further cultured with the human ABC differentiation cocktail. On day 4, cells were analyzed by flow cytometry. (**c**) Flow cytometry plots of ABCs ($CD27^-IgD^-CD11c^+T\text{-}bet^+$). Human B cells were activated and then were electroporated with Cas9-RNP targeting indicated gene described as in **b**. (**d-e**) Flow cytometry plots (**d**) and statistical analysis (**e**) of cell viability of B cells electroporated with Cas9-RNP targeting indicated gene and cultured with the human ABC differentiation cocktail. n refers to the measurement of distinct samples (biological repeats). Data are representative of 3 independent experiments. Bars indicate mean ± SEM values. Statistical significance determined by Student's t test.*$p < 0.05$, **$P < 0.01$, ***$P < 0.001$, ns, not significant.

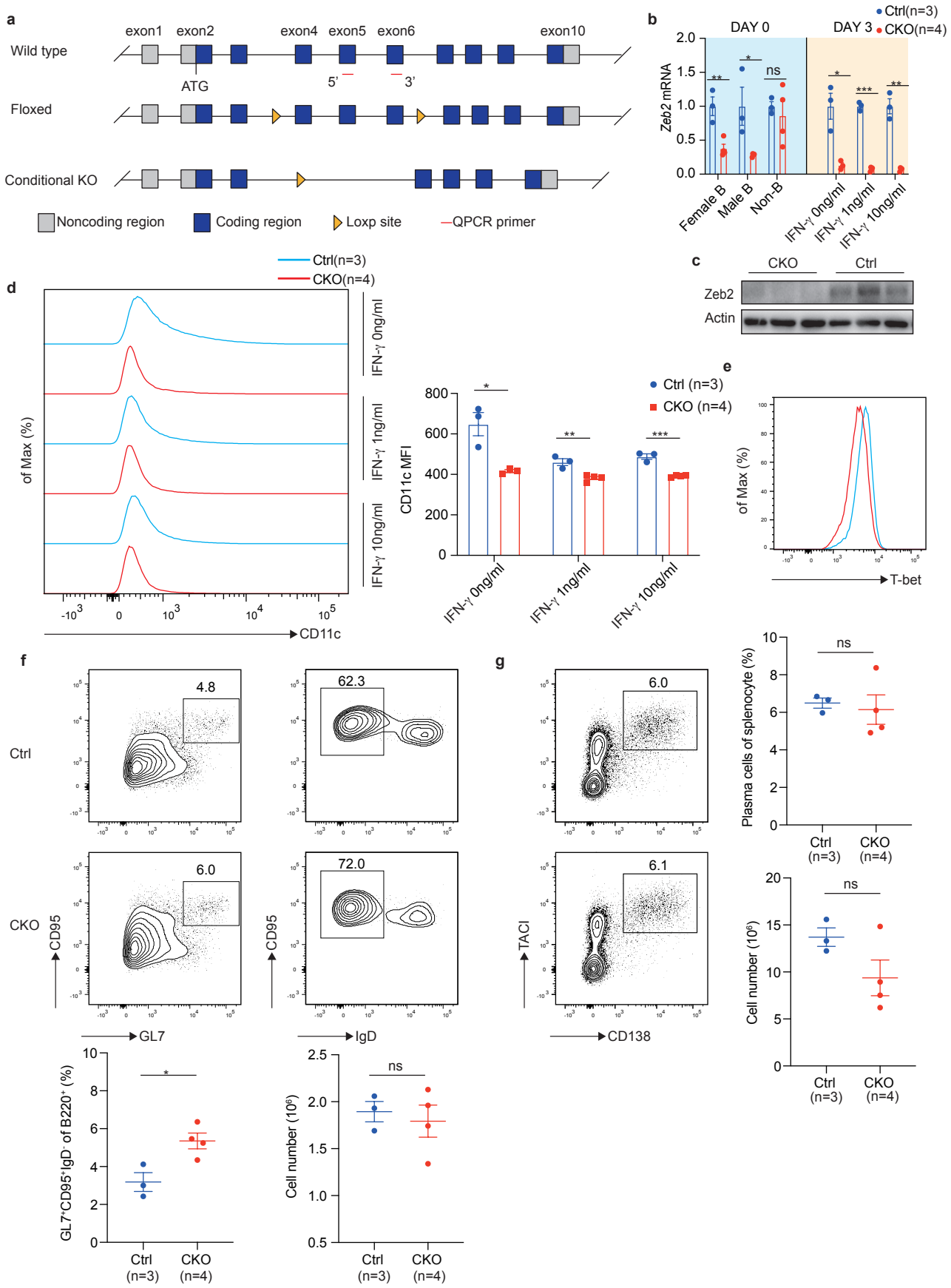

Extended Data Fig. 6 Impaired ABC formation in Zeb2 KO B cells.
(**a**) Schematic diagram for construction of Zeb2 conditional knockout allele: Exon 4 to 6 are chosen as a target for inserting Loxp sites by CRISPR/Cas9 technology. The floxed mice was crossed with mice expressing Cre recombinase. QPCR primers to detect *Zeb2* expression are labeled in red. (**b**) QPCR analysis of *Zeb2* expression in splenic B cells and non-B cell fractions (Day 0) or culture for 3 days described as in **Fig. 3a**. (**c**) Western blot analysis of Zeb2 protein level in splenic B cells from Zeb2 CKO and Ctrl mice. (**d-e**) Flow cytometry and statistical analysis of CD11c (**d**) and T-bet (**e**) of B cells from Ctrl and CKO mice and cultured for 3 days described as in **Fig. 3a**. (**f**) Flow cytometry plots and statistical analysis of splenic germinal center B cells ($IgD^-GL\text{-}7^+CD95^+$), plasma cells ($TACI^+CD138^+$) in Zeb2 CKO and Ctrl mice at week 2 after Bm-12 induction described as in **Fig. 3b**. n refers to the measurement of distinct samples (biological repeats). Data are representative of 2 independent experiments. Bars indicate mean ± SEM values. Statistical significance determined by Student's t test.*p < 0.05, **P < 0.01, ***P < 0.001, ns, not significant.

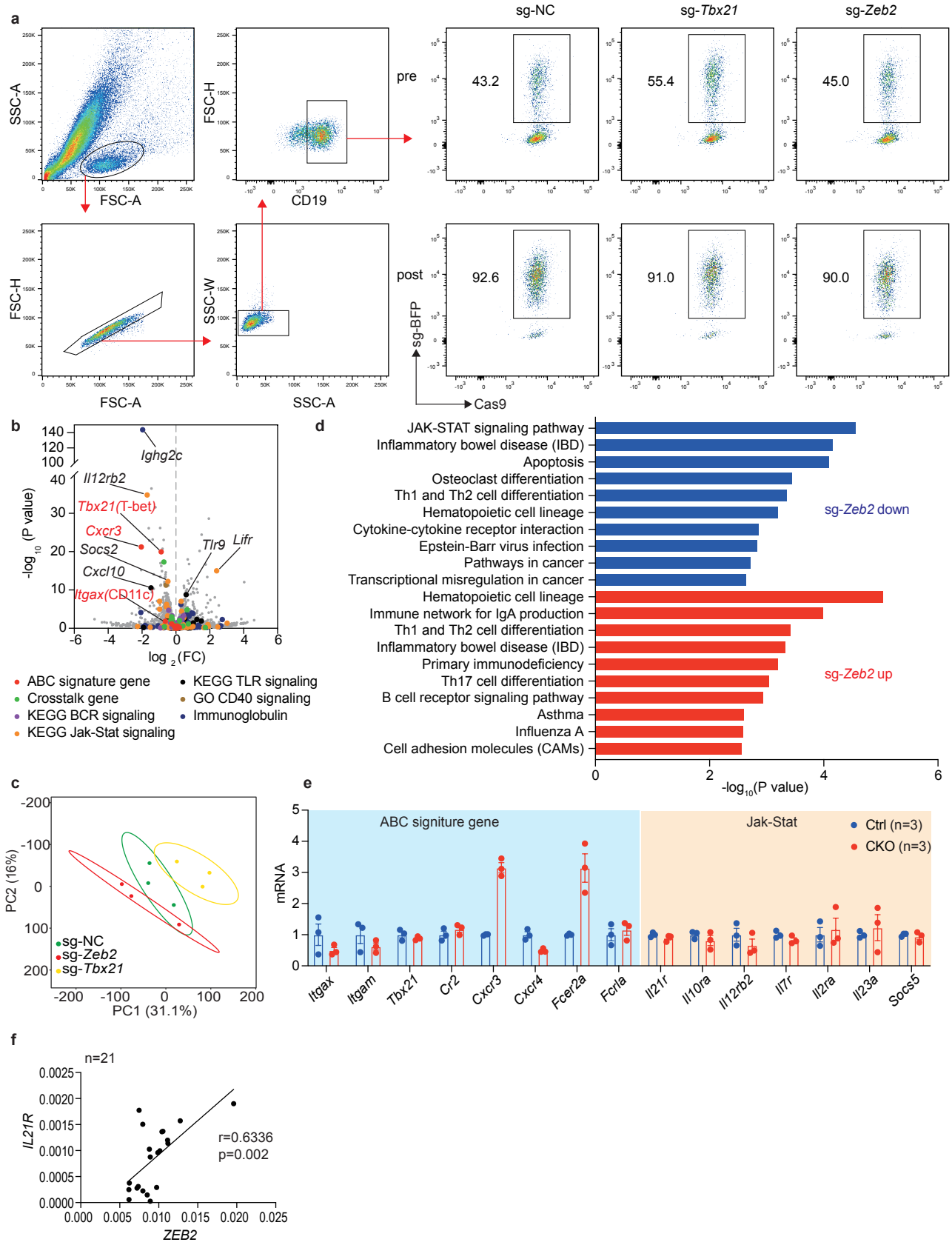

Extended Data Fig. 7 Zeb2 regulates ABC differentiation by targeting Jak-Stat.
(**a**) Cas9^{+} B cells were activated, retroviral infected with sg-RNA plasmid targeting *Tbx21* and *Zeb2* and cultured with the mouse ABC differentiation cocktail for 3 days. Infected B cells (CD19^{+}GFP^{+}BFP^{+}) were sorted by flow cytometry with enriched efficiency >90%. (**b**) Volcano graph showing the transcriptional profiles in mouse B cells edited by sg-NC and sg-*Tbx21* described as in **a**. ABC signature genes, Immunoglobulin genes, genes of BCR, TLR, Jak-Stat signaling from KEGG database, GO CD40 signaling and crosstalk genes were labeled with colored dots. (**c**) Principal component analysis (PCA) of protein coding genes from RNA-seq data described as in **a**. (**d**) KEGG pathway enrichment analysis of downregulated genes (blue) and upregulated genes (red) in sg-*Zeb2* B cells was performed by online Enrichr tools. P-values was log-normalized. (**e**) Splenic B cells were isolated from Zeb2$^{flox/flox}$ CD19$^{+/+}$(Ctrl) and Zeb2$^{flox/flox}$ CD19$^{Cre/+}$(CKO) mice and cultured cultured with the mouse ABC differentiation cocktail for 3 days. QPCR validation of selected ABC signature genes and Jak-Stat signaling genes. (**f**) Correlation analysis of *ZEB2* mRNA expression with *IL21R* in peripheral B cells of SLE patients. n refers to the measurement of distinct samples (biological repeats). Data are representative of 2 independent experiments in **e**. Bars indicate mean ± SEM values. Statistical significance determined by Student's t test.*p < 0.05, **P < 0.01, ***P < 0.001, ns, not significant.

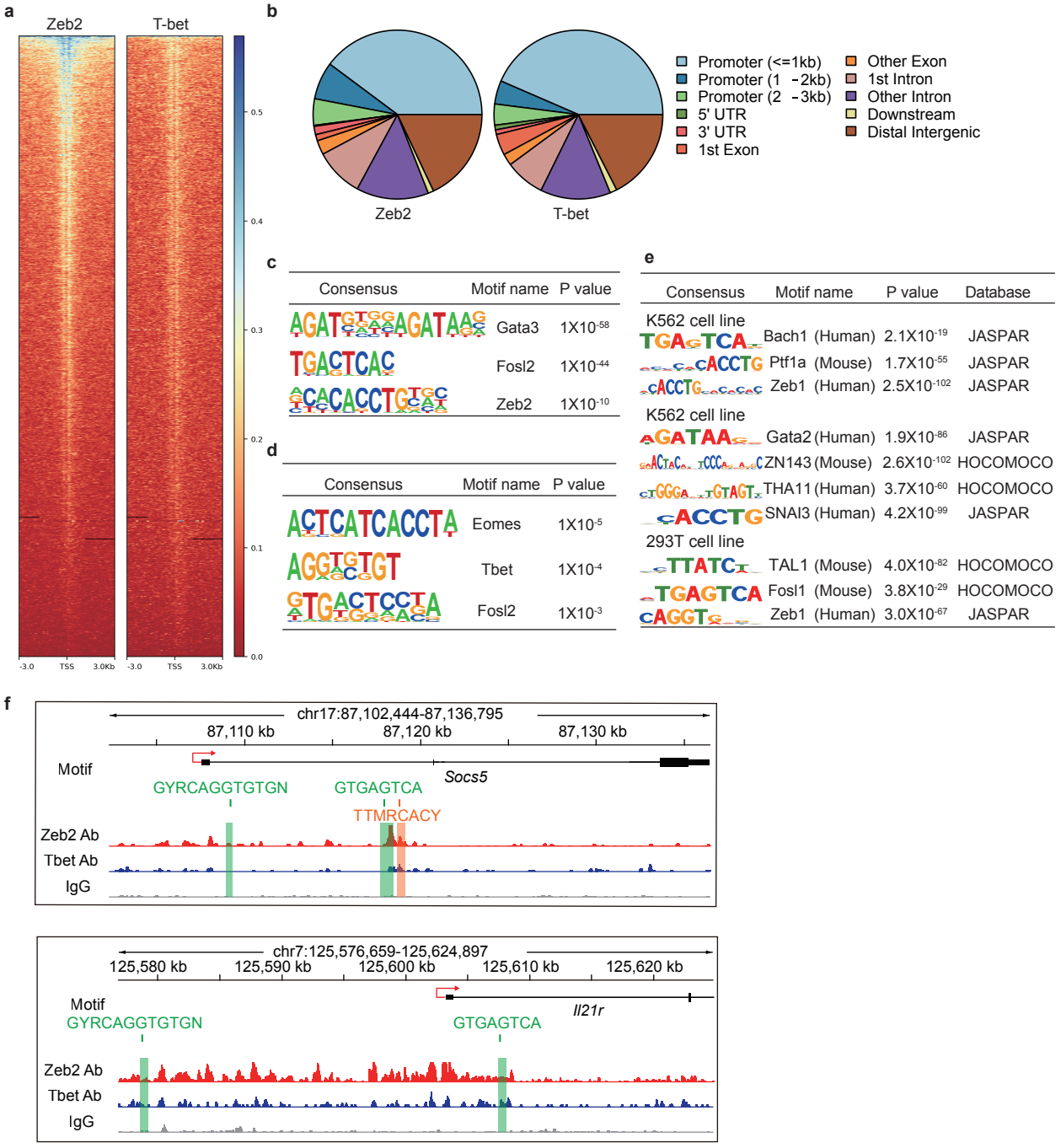

Extended Data Fig. 8 Zeb2 directly binds to promoter regions of *Il21r* and *Socs5*.
(**a**) Heatmap graph showing distributions of Zeb2 and T-bet specific singaling. The horizontal axis represented the normalized gene range coordinates. (**b**) Peak annotation analysis of distribution of T-bet and Zeb2 in the functional area of gene covered. (**c-d**) Motif-enrichment analysis of Zeb2 (**c**) or T-bet (**d**) specific peaks generated from CUT&Tag sequencing data.(**e**) Motif analysis of Zeb2 specific peak of Chip-seq data in cell lines from Encode project.(**f**) IGV trunk view of OCR signals in transcriptional regulatory regions of *Socs5* and *Il21r*. IgG (gray line), Zeb2 (red line) and T-bet (blue line) specific signals at indicated loci were shown. Consensus Zeb2 (green) and T-bet (orange) binding motifs within the differentially accessible regions were indicated.

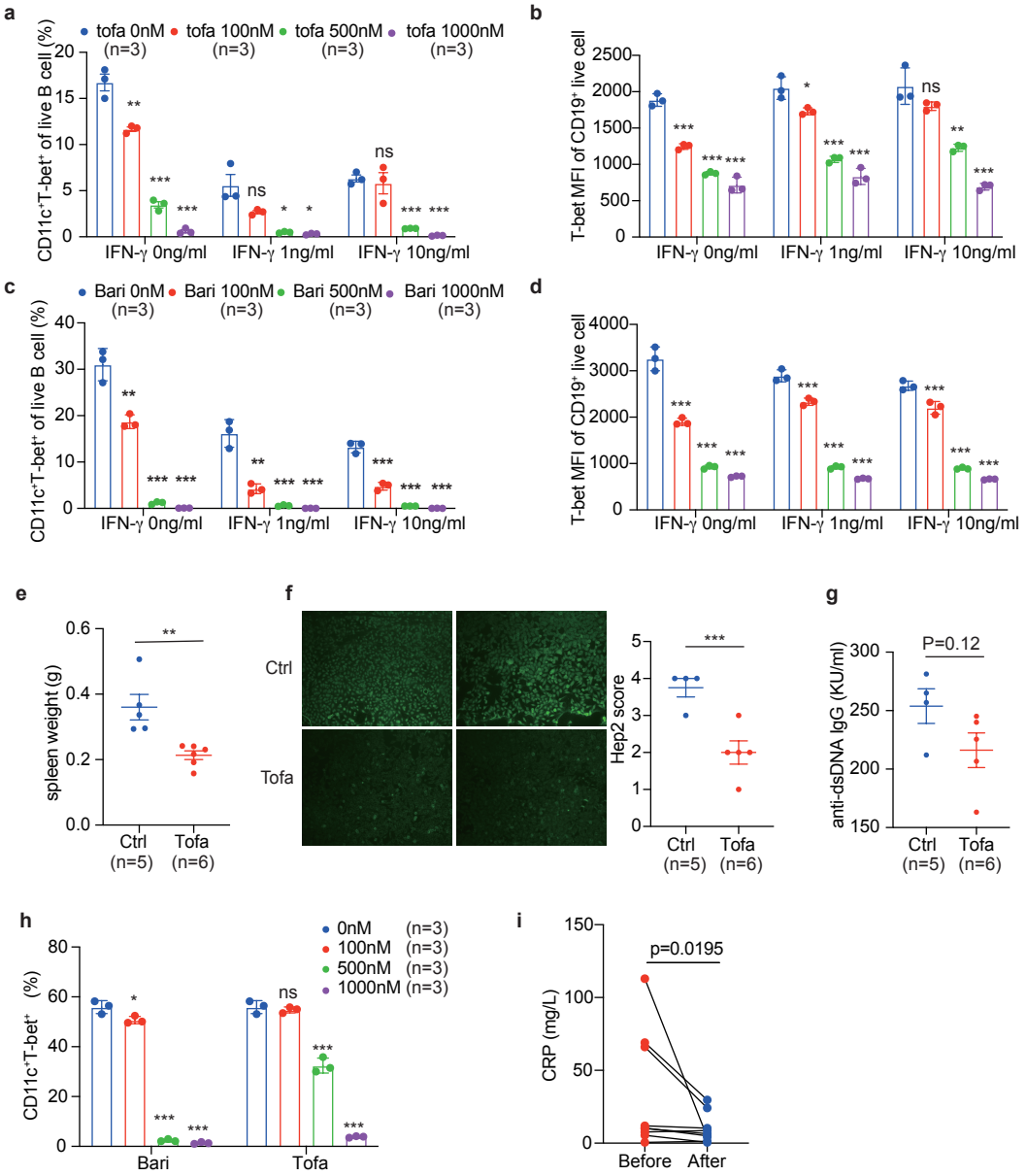

Extended Data Fig. 9 Jak-stat inhibitors impair ABC formation.
(**a, c**) Statistical analysis of mouse ABCs (CD11c$^+$T-bet$^+$) generated from in vitro induction with different concentration (mock, 100 nM, 500 nM and 1000 nM) of tofacitinib (**a**) or baricitinib (**c**). (**b,d**) T-bet MFI of B cells generated from in vitro induction with different concentration (mock, 100 nM, 500 nM and 1000 nM) of tofacitinib (**b**) or baricitinib (**d**). (**e-g**) C57 mice injected with CD4$^+$ T cells from Bm12 mice were treated with tofacitinib 30 mg/kg once a day by oral gavage for 2 weeks and then sacrificed to analyze spleen weight (**e**), ANA (**f**) and anti-dsDNA (**g**) in serum.(**h**) Statistical analysis of in vitro induced human ABCs (CD11c$^+$T-bet$^+$) with different concentration (mock, 100 nM, 500 nM and 1000 nM) of baricitinib or tofacitinib. (**i**) CRP level in RA patients before and after tofacitinib treatment for 4 weeks. n refers to the measurement of distinct samples (biological repeats). Data are representative of 3 independent experiments in **e-h**. Bars indicate mean ± SEM values. Statistical significance determined by Student's t test.*p $<$ 0.05, **P $<$ 0.01, ***P $<$ 0.001, ns, not significant.

Supplemental Table 1. Basic clinical characteristics of a patient with new-onset SLE

	SLE patient
Age	27
Sex	Female
WBC ($\times 10^9$/L)	4.35
RBC ($\times 10^{12}$/L)	3.14
Hb(g/L)	106
PLT($\times 10^9$/L)	212
ESR(mm/h)	82
IgA(g/L)	4.23
IgM(g/L)	1.5
IgG(g/L)	26.5
C3(g/L)	0.149
C4(g/L)	<0.017
Anti-dsDNA(IU/ml)	292.16
SLEDAI	24
ANA	Positive
Anti-SSA	Negative
Anti-SSB	Negative
Anti-U1RNP	Negative
Anti-Sm	Negative
Anti-rRNP	Positive
Anti-ANUA	Positive
ACL	Positive
Fever	No
Rash	Yes
Alpecia	Yes
Arthritis	No
Oral ulcers	No
Cutaneous vasculitis	No
Raynaud's	No
Leukopenia and/or Thrombocytopenia	No
Anemia	No
Serositis	No
NPSLE	No
LN	III+V
Urine protein of LN patients (mg/24h)	3379.8

Supplemental Table 2. Basic clinical characteristics of the SLE cohort

	SLE patients (n=21)
Female(%)	20(0.95)
Age, years	32(20-70)
SLEDAI	12(0-22)
Anti-dsDNA (U/ml)	32.13(7.06-100)
C3(g/L)	0.646(0.218-1.25)
C4(g/L)	0.11(0.018-0.343)
ESR(mm/h)	26(1-99)
CRP(mg/L)	3.3(0.2-62.2)
ANA^+(%)	20(0.95)
Anti-Sm^+(%)	5(0.24)
Anti-SSA^+(%)	11(0.52)
Anti-SSB^+(%)	5(0.24)
Anti-RNP^+(%)	6(0.29)
LN(%)	12(0.57)
24-urine protein (mg/24h)	2336.3(88.6-14900.7)

Supplemental Table 3. Clinical characteristics of RA patients treatment with tofacitinib

RA patients	Before (n=6)	After (n=6)
WBC($\times 10^9$/L)	6.30±2.92	6.30±2.03
RBC($\times 10^{12}$/L)	4.73±0.56	4.70±0.62
Hb(g/L)	136±25.25	137±23.50
PLT($\times 10^9$/L)	322±127.5	274±120
ESR(mm/h)	28±25.88	19±11.00
CRP(mg/L)	10.4±32.80	6.6±4.90
Cr(μmol/L)	56.2±8.93	62.2±13.85
ALT(U/L)	21±11.25	25±7.00

Supplemental Table 4. List of antibodies

Antibodies	Source	Identifier
anti-mouse CD4	biolegend	Clone GK1.5
anti-mouse CD8	biolegend	Clone 53-6.7
anti-mouse CD19	biolegend	Clone 6D5
anti-mouse CD19	biolegend	Clone 1D3/CD19
anti-mouse CD44	BD bioscience	Clone IM7
anti-mouse CD62L	BD bioscience	Clone MEL-14
anti-mouse PD-1	eBioscience	Clone J43
anti-mouse B220	biolegend	Clone RA3-6B2
anti-mouse CD95	BD bioscience	Clone Jo2
anti-mouse GL-7	BD bioscience	Clone GL7
anti-mouse IgM	BD Bioscience	Clone R6-60.2
anti-mouse IgD	BD Bioscience	Clone 11-26c.2a
anti-mouse CD138	biolegend	Clone 281-2
anti-mouse TACI	biolegend	Clone 8F10
anti-mouse CD11c	biolegend	Clone N418
anti-mouse/human T-bet	biolegend	Clone 4B10
anti-mouse CD21	biolegend	Clone 7E9
anti-mouse CD73	biolegend	Clone TY/11.8
anti-mouse CD80	biolegend	Clone 16-10A1
anti-mouse CD93	BD Bioscience	Clone AA4.1
anti-mouse CD45.1	biolegend	Clone A20
anti-mouse CD86	BD bioscience	Clone GL1
anti-mouse I-A/I-E	BD bioscience	Clone M5/114.15.2
anti-mouse CD23	BD bioscience	Clone B3B4
anti-mouse CD11b	biolegend	Clone M1/70
anti-mouse CD5	eBioscience	Clone 53-7.3
anti-mouse CXCR4	BD Bioscience	Clone 2B11/CXCR4
anti-mouse CXCR3	biolegend	Clone CXCR3-173
anti-human CD19	biolegend	Clone HIB19
anti-human CXCR5	biolegend	Clone J252D4
anti-human IgD	biolegend	Clone IA6-2
anti-human CD27	biolegend	Clone M-T271
anti-human CD11c	biolegend	Clone S-HCL-3
anti-human CD38	biolegend	Clone HIT2
anti-human CD21	biolegend	Clone Bu32
Biotin Rat Anti-Mouse CD185 (CXCR5)	BD bioscience	Clone 2G8
Zombie Aqua™ Fixable Viability Kit	biolegend	Cat#423102
PE Streptavidin	BD bioscience	Cat#554061
T-bet (4B10) Antibody	Santa Cruz Biotechnology	Cat#sc-21749
ZEB2 antibody	Novus	Cat#NBP1-82991

Supplemental Table 5. List of sgRNA sequence

Gene name	Sg sequence(5'-3')
mouse	
Zeb2 Sg1	GTACCTTCAGCGAAGCGACA
Zeb2 Sg2	TATGAATAGTAACTTGAGTG
T-bet	CGAGGACTACGCATTGCCCG
Itgax	GGGCCGTAACTCACCCTGGA
Zbtb32	CGAGGTATCGAGAGCCACAA
Tfeb	CCTCTGTGGATTACATCCGG
Litaf	GATAACAGACATACTTGCGT
Nfatc2	TTGGAGAGTGGCCACTCGAG
Srebf2	ACTCCAGTGACAGTACACTG
Jazf1	CACAGGCAGCGAGTATGATG
Jun	TGTGCCGCGGAGGTGACACT
Plek	GTTTGCCAAAGTCTTGACAA
Batf	AGAGATCAAACAGCTCACCG
Tfec	CATCAGTGGACTACATCAAG
Sox5	CGAGGGTCCGCTGGTCAGGA
Mbd4	TCAGAGTCGCCAGAAAGCAG
Ets1	TGCCTGGGGAGAGCCAGTCG
Fli1	TCACGACTGAATGTCAAGGA
human	
ZEB2 Sg1	TTGTAGCCCCGGTCGCAGTA
ZEB2 Sg2	GGCGCAAACAAGCCAATCCC
TBX21	AAACCGCCTGTACGTCCACC
BATF	AGGACTCTACCTGTTTGCCA
FLI1	ACTCAATCGTGAGGATTGGT
SREBF2	GCTGCATTCTGGTATATCAA
ETS1	CTTACTAATGAAGTAATCCG
JUN	TGAACCTGGCCGACCCAGTG
CD19	CTGTGCTGCAGTGCCTCAA

Supplemental Table 6. List of primers

	Gene name	Forward	Reverse
Mouse			
	Hopx	5'- CAACTTCAACAAGGTCAACAAGCAC-3'	5'-ACCATTTCTGCGTCTGCTCCT-3'
	Zeb2	5'-GCAGTGAGCATCGAAGAGTACC-3'	5'-GGCAAAAGCATCTGGAGTTCCAG-3'
	Tbx21	5'-TGTGGATGTGGTCTTGGTGG-3'	5'-ATTGTTGGAAGCCCCCTTGT-3'
	Cd11c	5'-TTGGCTTGTGGTCCTACTGTG-3'	5'-GGGAAGTTCTGGCTCTGCTTG-3'
	Cd11b	5'-GTGAATATGTCCTTGGGCCTGT -3'	5'-CGGAGCCATCAATCAAGAAGACA -3'
	Zbtb32	5'-TCCAGATACGGTGCTCCCTTCT-3'	5'-CCAGAGAGCTTTGGAGTGGTTC-3'
	Il7r	5'-CACAGCCAGTTGGAAGTGGATG-3'	5'-GGCATTTCACTCGTAAAAGAGCC-3'
	Cxcl10	5'-ATCATCCCTGCGAGCCTATCCT-3'	5'-GACCTTTTTTGGCTAAACGCTTTC-3'
	Cxcr3	5'-TACCTTGAGGTTAGTGAACGTCA-3'	5'-CGCTCTCGTTTTCCCCATAATC-3'
	Il2ra	5'-GCGTTGCTTAGGAAACTCCTGG-3'	5'-GCATAGACTGTGTTGGCTTCTGC-3'
	Rp13a	5'-GGGCAGGTTCTGGTATTGGAT-3'	5'-GGCTCGGAAATGGTAGGGG-3'
	Cxcl9	5'-AATGCACGATGCTCCTGCA-3'	5'-AGGTCTTTGCGGGATTTGTAGTGG-3'
	Bach2	5'-ACAGACGAAAGATGACTTGGTG-3'	5'-CTCTGCTGAGTAACAGCTTGG-3'
	Myc	5'-ACGGCCTTCTCTCCTTCCTC-3'	5'-GCCTCTTCTCCACAGACACC-3'
	Nfatc2	5'-TCATCCAACAACAGACTGCCC-3'	5'-GGGAGGGAGGTCCTGAAAACT-3'
	Junb	5'-TCACGACGACTCTTACGCAG-3'	5'-CCTTGAGACCCCGATAGGGA-3'
	Jun	5'-CCTTCTACGACGATGCCCTC-3'	5'-GGTTCAAGGTCATGCTCTGTTT-3'
	Srebf2	5'-AGAAAGAGCGGTGGAGTCCTTG-3'	5'-GAACTGCTGGAGAATGGTGAGG-3'
	Foxp1	5'-CATGCCTCTACCAATGGACAGC-3'	5'-GAAGTCGTCACAAACCGCCTCA-3'
	Zfp36l1	5'-CTTCCACACCATCGGCTTTTGC-3'	5'-CACTGGGAAACCCAGCAAAGCT-3'
	Aff3	5'-AGATGACCTGGCTTCCTCCACT-3'	5'-GTCCAGAGGATACAAGTTGCGAG-3'
	Tfeb	5'-CCACCCCAGCCATCAACAC-3'	5'-CAGACAGATACTCCCGAACCTT-3'
	Klf6	5'-GGAAGGTTGTGAGTGGCGTTTTG-3'	5'-AGGTGGTCAGACCTGGAGAAAC-3'
	Irf1	5'-TCCAAGTCCAGCCGAGACACTA-3'	5'-ACTGCTGTGGTCATCAGGTAGG-3'
	Irf8	5'-CAATCAGGAGGTGGATGCTTCC-3'	5'-GTTCAGAGCACAGCGTAACCTC-3'
	Pou2f2	5'-TCCTGGAGAAGTGGCTCAACGA-3'	5'-ATGCTGGTCCTCTTCTTGCGTC-3'
	Litaf	5'-CAAGATGATCGTGACCCAGCTG-3'	5'-GCAGTAGTGGTCCACATCCTGT-3'
	Klf3	5'-CCTCTCATGGTTTCCTTGTCGG-3'	5'-CCTCTGTGGTTCAATTCCAGGC-3'
	Jazf1	5'-CGACATAGCAGTGGCAGCCTTA-3'	5'-TCTCTGTGGTCCAGGACTCATC-3'
	Plek	5'-GGAGCAGTTCACTTGAGAGGCT-3'	5'-TGGAAGTGGCTGCCTGCAAGTA-3'
	Plscr1	5'-GACCTCTGAGATGCAGTAGCTG-3'	5'-GGAGAGTGAACTTGGGCAGACA-3'
	Zfp36l2	5'-AAGTACGGCGAGAAGTGCCAGT-3'	5'-AGAAGCCGATGGTGTGGAAGGT-3'
	Fos	5'-AGGGGCAAAGTAGAGCAGCTA-3'	5'-CAATCTCAGTCTGCAACGCA-3'
	Prdm1	5'-AAGAGGTTATTGGCGTGGTAAG-3'	5'-TAGACTTCACCGATGAGGGGT-3'
	Irf4	5'-CTTTGAGGAATTGGTCGAGAGG-3'	5'-GAGAGCCATAAGGTGCTGTCA-3'
	Tox	5'-AAGATGGCGCACTGCTCTCCAA-3'	5'-CATGCTTGCCTGCTGTCTGATG-3'
	Bhlhe40	5'-CGGATTAACGAGTGCATTGCCC-3'	5'-GCTTCAACGTAAGCTCCAGAACC-3'
	Foxp4	5'-CACCAGGATGTTCGCCTACTTC-3'	5'-TATTCCCGCTCATCCACAGTCC-3'
	Sox5	5'-CGCCAGATGAAAGAGCAACTCAG-3'	5'-TGAGTCAGGCTCTCCAGTGTTG-3'
	Crem	5'-GCAGCACAATCAGCCGATGGTA-3'	5'-AGCTCGGATCTGGTAAGTTGGC-3'
	Arid5a	5'-CGCCTCTGGAAGAACGTGTATG-3'	5'-TGGTAGGAGGCAGTGGCTTGTC-3'
	Arid3a	5'-TCCATCACCAGTGCTGCCTTCA-3'	5'-TCCCTGCGATTGCTGTCTATGG-3'
	Fli1	5'-CCATACAGACCAGTCCTCACGA-3'	5'-CATGGTCTGTGATCCTCCAAGG-3'
	Mbd4	5'-ACAGGATGGCTCTGAAATGCCC-3'	5'-ACTTGTGTCCGTGGGATGCTGT-3'
	Ets1	5'-CCAGAATCCTGTTACACCTCGG-3'	5'-CAGCGTCTGATAGGACTCTGTG-3'
	Hif1a	5'-CCTGCACTGAATCAAGAGGTTGC-3'	5'-CCATCAGAAGGACTTGCTGGCT-3'
	Il-12rb2	5'-TTGGACGGCATCAGTGTCTGCA-3'	5'-TCCGACTTTGCAGAGACCTGGT-3'
Human			
	ZEB2	5'-AATGCACAGAGTGTGGCAAGGC-3'	5'-CTGCTGATGTGCGAACTGTAGG-3'
	IL-21R	5'-ACCAGTCTGGCAACTACTCCCA-3'	5'-AGGGTCTTCGTAATCTGAGCGC-3'
	RPL13A	5'-CGAGGTTGGCTGGAAGTACC-3'	5'-CTTCTCGGCCTGTTTCCGTAG-3'